Article

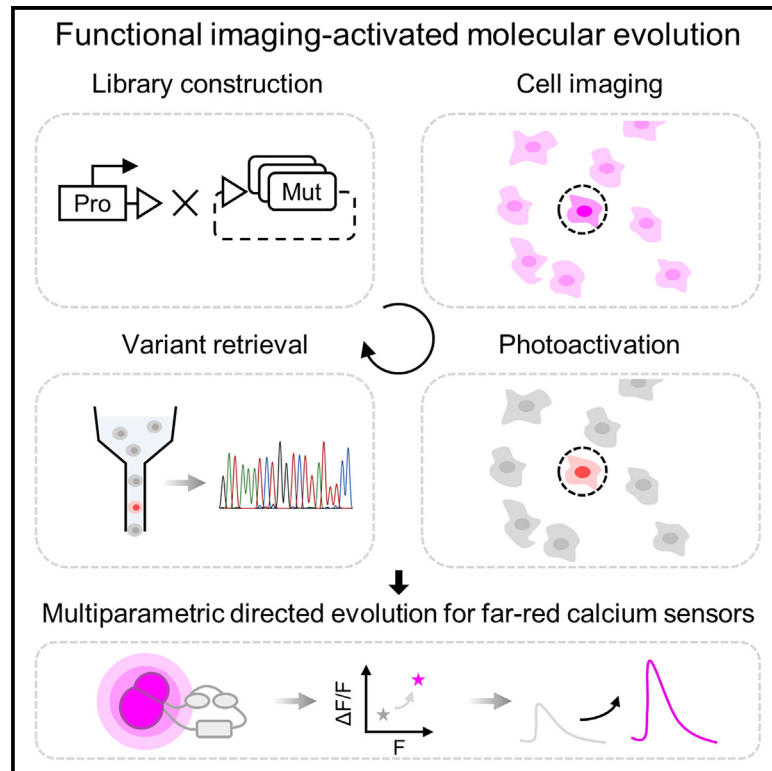# Functional imaging-guided cell selection for evolving genetically encoded fluorescent indicators

Graphical abstract

Highlights

- Development of a microscopy imaging-guided cell selection strategy, Faculae

- Recombinase-assisted mutant library preparation

- Multidimensional directed evolution of far-red fluorescent calcium indicators

- Nier1 indicators exhibit improved brightness and sensitivity in neurons

Authors

Chang Lin, Lihao Liu, Peng Zou

Correspondence

zoupeng@pku.edu.cn

In brief

Lin et al. develop an imaging-guided pooled library screening platform that evaluates tens of thousands of variants in cultured mammalian cells in a single run. Cells of interest are phototagged and recovered via flow cytometry for genotyping. This screening platform supports the directed evolution of genetically encoded fluorescent indicators, such as far-red calcium indicators.

CellPress

Article

Functional imaging-guided cell selection for evolving genetically encoded fluorescent indicators

Chang Lin,[1] Lihao Liu,[1] and Peng Zou[1,2,3,4,*]
[1]College of Chemistry and Molecular Engineering, Synthetic and Functional Biomolecules Center, Beijing National Laboratory for Molecular Sciences, Key Laboratory of Bioorganic Chemistry and Molecular Engineering of Ministry of Education, Peking University, Beijing 100871, China
[2]Academy for Advanced Interdisciplinary Studies, PKU-Tsinghua Center for Life Science, PKU-IDG/McGovern Institute for Brain Research, Peking University, Beijing 100871, China
[3]Chinese Institute for Brain Research (CIBR), Beijing 102206, China
[4]Lead contact
*Correspondence: zoupeng@pku.edu.cn
https://doi.org/10.1016/j.crmeth.2023.100544

MOTIVATION Genetically encoded fluorescent indicators enable the non-invasive optical recording of cellular activities. Engineering these indicators often requires the simultaneous assessment of multiple key parameters such as brightness, sensitivity, and response kinetics. Herein, we report the design and implementation of a microscopic imaging-guided cell selection technology that can evaluate multiple parameters in a mammalian cell population and screen 10^4-10^5 variants at a time.

SUMMARY

Genetically encoded fluorescent indicators are powerful tools for tracking cellular dynamic processes. Engineering these indicators requires balancing screening dimensions with screening throughput. Herein, we present a functional imaging-guided photoactivatable cell selection platform, Faculae (functional imaging-activated molecular evolution), for linking microscopic phenotype with the underlying genotype in a pooled mutant library. Faculae is capable of assessing tens of thousands of variants in mammalian cells simultaneously while achieving photoactivation with single-cell resolution in seconds. To demonstrate the feasibility of this approach, we applied Faculae to perform multidimensional directed evolution for far-red genetically encoded calcium indicators (FR-GECIs) with improved brightness (Nier1b) and signal-to-baseline ratio (Nier1s). We anticipate that this image-based pooled screening method will facilitate the development of a wide variety of biomolecular tools.

INTRODUCTION

Genetically encoded fluorescent indicators are powerful tools for monitoring the dynamics of cellular physiology. Among these, fluorescent protein (FP)-based intensiometric biosensors are particularly significant due to their large dynamic ranges and good spectra compatibility for multiplexed imaging. Therefore, they have been widely used in recording neural activities, including neurotransmitter release,[1] calcium ion dynamics,[2] and membrane potential fluctuations.[3]

Assessment of fluorescent indicators typically includes key parameters such as brightness, signal-to-baseline ratio ($\Delta F/F_0$), dynamic range (F_{max}/F_{min}), photostability, protein stability, etc. Improving indicator performance on these fronts often requires labor-intensive protein engineering and screening efforts.

Notably, there is a general trade-off between screening throughput and the number of parameters being evaluated in single-trial measurements. For example, fluorescence-activated cell sorting (FACS)-based screens can evaluate brightness of FP libraries larger than 10^6 in a single run[4] but are incapable of measuring dynamic parameters such as dynamic range of biosensors in individual cells. Array-based screens, such as those performed in multiwell plates, enable both static and dynamic signal detection but are usually limited to the screening of thousands of mutants at a time and require laborious procedures to prepare the library.[5–7] Recently, microscope-based pooled screens have been applied for linking the visually examined phenotypes to the genotypes of pooled variants,[8–13] which are well suited for high-throughput biosensor screening owing to their abilities to measure dynamic parameters with high

spatiotemporal resolution, while simultaneously acquiring genetic information on promising candidate mutants.

Several microscopy-based pooled screening platforms have been recently developed to engineer genetically encoded fluorescent indicators.[14,15] In these methods, cultured cells expressing a library of biosensor mutants are initially evaluated under a fluorescence microscope. Thereafter, target cells with desired properties (e.g., improved brightness, SBR, photostability, etc.) are identified and retrieved for genotyping, either by fluorescent tagging and subsequent cell sorting or by direct aspiration from the plate. For example, Photopick utilized patterned illumination to phototag target cells expressing a green-to-red photoconvertible FP, which were subsequently sorted with flow cytometry. This method has been successfully employed to screen far-red genetically encoded voltage indicators in engineered HEK 293T cells.[14] One limitation of Photopick is its requirement of using a green-to-red photoconvertible FP marker, which impedes its application to GFP- or RFP-based indicators. In another approach, termed Opto-MASS, genetically encoded neurotransmitter indicators in mammalian cell libraries are screened in microwell array formats, with identified high-ranking cells aspirated by micropipettes.[15] This aspiration-based retrieval method is time consuming and low throughput. Therefore, a generalizable and automated microscopy-based cell selection method is still needed.

Far-red genetically encoded calcium indicators (FR-GECIs) have become promising tools for deep-tissue imaging and multiplexed imaging due to their FR spectral property.[16–18] Recently, a series of intensiometric FR-GECIs (termed near-infrared genetically encoded Ca^{2+} indicator for optical imaging, abbreviated as NIR-GECOs) have been developed that consist of a calcium-binding domain, calmodulin (CaM)-RS20, inserted into a monomeric infrared FP (mIFP).[17,18] However, NIR-GECOs still suffer from low molecular brightness and limited fluorescence response and require further improvement in both dimensions.

Herein, we report a microscopic imaging-guided pooled screening strategy, termed functional imaging-activated molecular evolution (Faculae), that can, in principle, be used for the evolution of a wide variety of fluorescent indicators. First, we construct biosensor libraries in mammalian cells efficiently through recombinase-based locus-specific integration. Then, we screen the pooled library under the microscope, followed by photoactivating the target cell population via focused illumination with single-cell resolution and on a timescale of seconds per cell. Thereafter, phototagged candidate cells are retrieved by FACS for further genotyping. To demonstrate its capability, we applied Faculae to perform multidimensional screening of FR-GECIs and generated Nier1s and Nier1b with improved performance.

RESULTS

Characterization of imaging-guided cell selection platform

To enable cell selection under microscope, we achieved fast and precise optical labeling of target cells by photoactivating FPs through partially focused laser beam. Phototaggable (photoconvertible, activatable, or switchable) FPs have been applied as fluorescent markers for visualizable phenotypes in many studies.[19–21] Although the digital micromirror device (DMD) has

been widely used for spatially selective activation, it is generally time consuming to activate cells within each field of view due to low power density.[11] For the optical tagging of hundreds and thousands of cells, we reasoned that a focal illumination approach, which could restrict the photoactivating light directly on one cell, would be more efficient.[22] We filled the back aperture of the objective (20×, 0.75 NA) with a partially collimated 405 nm laser to generate a disc-like illumination pattern with a diameter of ~15 μm at the focal plane, with an estimated power density of 80 W/cm² at its center (Figures 1A, S1A, and S1B). To test the photoactivation kinetics, we expressed photoactivatable mCherry[23] (PAmCherry) in human embryonic kidney 293T (HEK 293T) cells. Under focal illumination, the fluorescence of PAmCherry in targeted cells increased by more than 100 times after 1.5 s activation, while the ratio of fluorescence intensity of targeted cells to neighboring cells reached a maximum of 50 ± 10 (mean ± SEM) at approximately 2.5 s (Figures 1B and 1C). We repeated the above experiment with PA-GFP,[24] whose intensity increased by 49-fold following 1 s activation with a focused 405 nm laser (Figure S1C). Taken together, the above characterization demonstrated the capability of activating either red or green fluorescence with single-cell spatial resolution and second-scale temporal resolution. We decided to use 1–1.5 s photoactivation for subsequent experiments to shorten the activation time and to reduce the off-target activation background.

We next tested the efficiency and specificity of retrieving photoactivated cells with FACS. We transiently expressed either GFP-P2A-PAmCherry (GFP+/PAmCherry+) or miRFP680-P2A-PAmCherry (miRFP680+/PAmCherry+) in two separate pools of HEK 293T cells. We randomly doped a small portion of GFP+/PAmCherry+ cells (5%) into miRFP680+/PAmCherry+ cells (95%) and co-cultured the mixed population in the glass-bottom dish. Under the microscopy, GFP+ cells were readily distinguishable from miRFP680+ ones both by visual examination and by automated image analysis (Figures 1D and 1E). We photoactivated 50–100 GFP+/PAmCherry+ cells with pulsed 405 nm laser spot illumination within a total of 4 min. Cells were lifted off the glass-bottom dish with trypsinization and sorted for mCherry+ cells by flow cytometry. Overall, we recovered 44% ± 8% (mean ± SD) of photoactivated cells with a precision of 96% ± 6% (defined as the ratio of true positives over the sum of true positives and false positives) (Figure 1F; Table S1), thus confirming that we can accurately activate and recover cells with the desired phenotype.

To achieve imaging-based pooled screening, we next tried to use a recombinase-based method to generate large-scale mutant libraries in mammalian cells.[25] Recombinase-based integration ensures the irreversible single-copy insertion of sequences at a pre-defined "landing-pad" locus within the mammalian cell genome (Figure 2A). To generate the lentiviral landing pad (LLP) cell line, we transduced LLP virus encoding either a CAG-attP or CMV-attP construct into HEK 293T cells at a low multiplicity of infection (MOI) and screened 16 clones (10 from the CAG construct and 6 from the CMV construct) with satisfactory expression level and high integration efficiency. Each LLP cell line was transfected with a mixture of attB-EGFP and attB-mCherry plasmids. All of these cell lines did not produce EGFP+/mCherry+ cells, confirming the single-locus
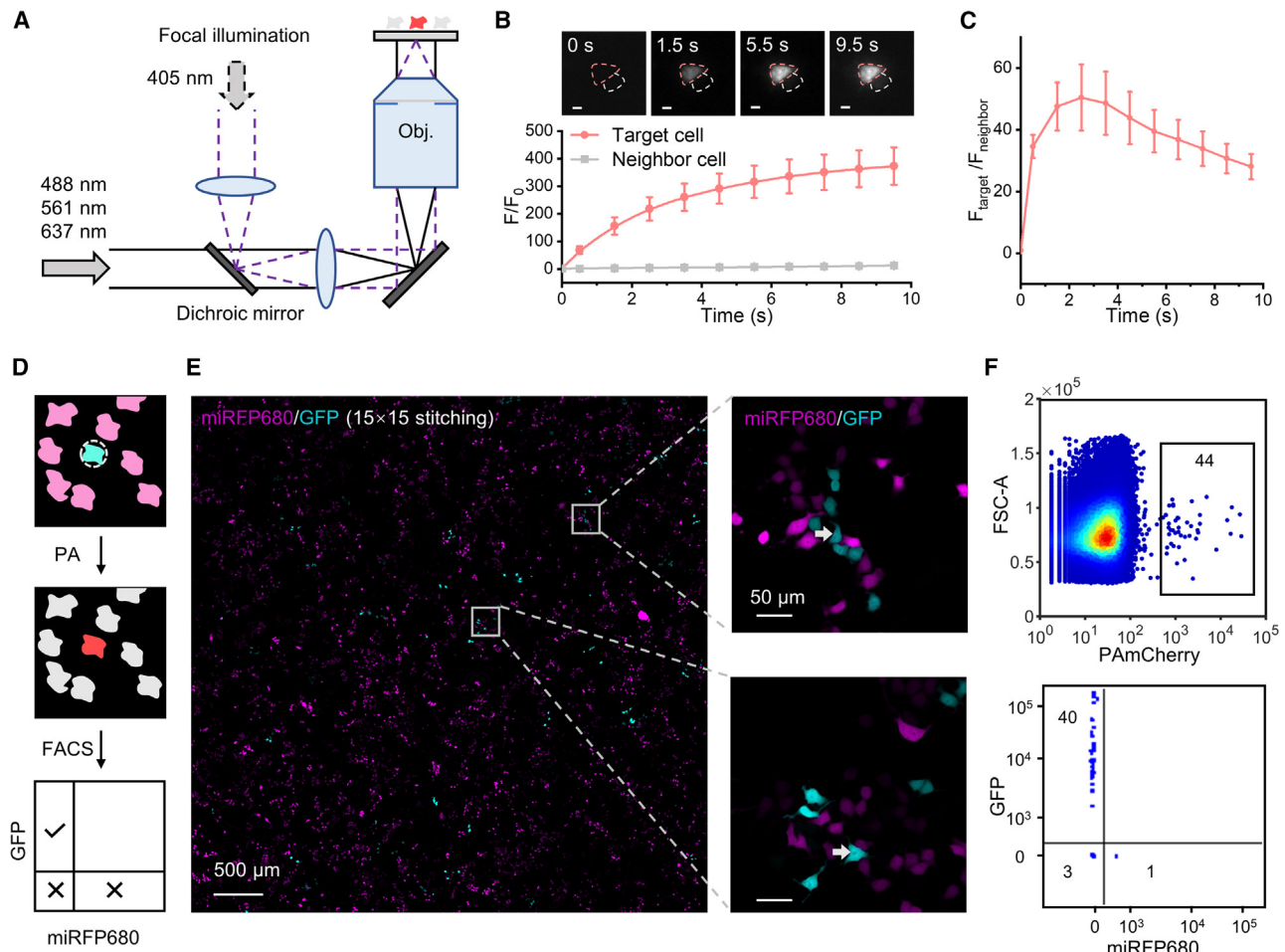
Figure 1. Faculae enabled precise photoactivation and retrieval of target cells

(A) Optical setup of focal illumination (violet dashed line) and wide-field imaging (black line).

(B) Target HEK 293T cells could be precisely photoactivated in seconds. In snapshots (first line), the red dashed line represents the target cell, and the gray dashed line represents the neighbor cell. Scale bar: 10 μm. $n_{target\ cell} = 15$; $n_{neighbor\ cell} = 15$. Error bars represent SEM.

(C) Fluorescence ratio ($F_{target}/F_{neighbor}$) peaked after around 2.5 s photoactivation. $n_{target\ cell} = 15$; $n_{neighbor\ cell} = 15$. Error bars represent SEM.

(D) HEK 293T cells transfected with GFP-P2A-PAmCherry were mixed with 20-fold more cells transfected with miRFP680-P2A-PAmCherry. GFP$^+$ cells were selected for photoactivation (PA) followed by FACS analysis.

(E) Tiled images and zoomed-in views of co-cultured cells expressing GFP or miRFP680. Gray arrows represent cells for activation.

(F) Top: 90 GFP$^+$ cells were optically activated while 44 cells were detected in the PAmCherry$^+$ gate during flow cytometry analysis. Bottom: 40 (~91%) were true positives (GFP$^+$ cells), while 4 were false positives (3 negative cells and 1 miRFP680$^+$ cell).

See also Figure S1 and Table S1.

---

integration (Figures S2A and S2B). By comparing the fluorescence intensity and the fraction of cells exhibiting single-integration (i.e., EGFP$^+$/mCherry$^-$ and EGFP$^+$/mCherry$^-$) cells, we identified one of the CAG clones with the highest expression level and the highest recombination efficiency (Figures S2B and S2C). We termed this cell line CAG-LLP and used it for constructing mutant libraries.

We evaluated the feasibility and throughput of Faculae by screening against an FR FP library. miRFP680 is an engineered monomeric FR FP derived from truncation of the *Rhodopseudomonas palustris* bacterial phytochrome photoreceptor RpBphP2, which consists of a Per-ARNT-Sim (PAS) domain and a cGMP phosphodiesterase/adenylate cyclase/FhlA (GAF)

domain with a pocket incorporating linear tetrapyrrole biliverdin IXa (BV) as a chromophore.[26] Two mutations, D202T and I203V, have been introduced into the conserved PXSDIP motif to increase the fluorescence quantum yield by stabilizing the chromophore.[26] We randomly mutated these two key residues and screened the mutant library for brightness with Faculae. A nuclear-localized EGFP was co-expressed and served both as a reference for expression level and a marker for facilitating image segmentation (Figures 2B and 2C). We screened over 4×10^4 cells under the microscope and photoactivated 117 cells (0.3%) exhibiting high brightness (Figures 2D–2F and S2D; Table S2). The screening-photoactivation process was completed within 1 h. Following FACS, 48 retrieved single cells were lysed, and 17 of them (35%)
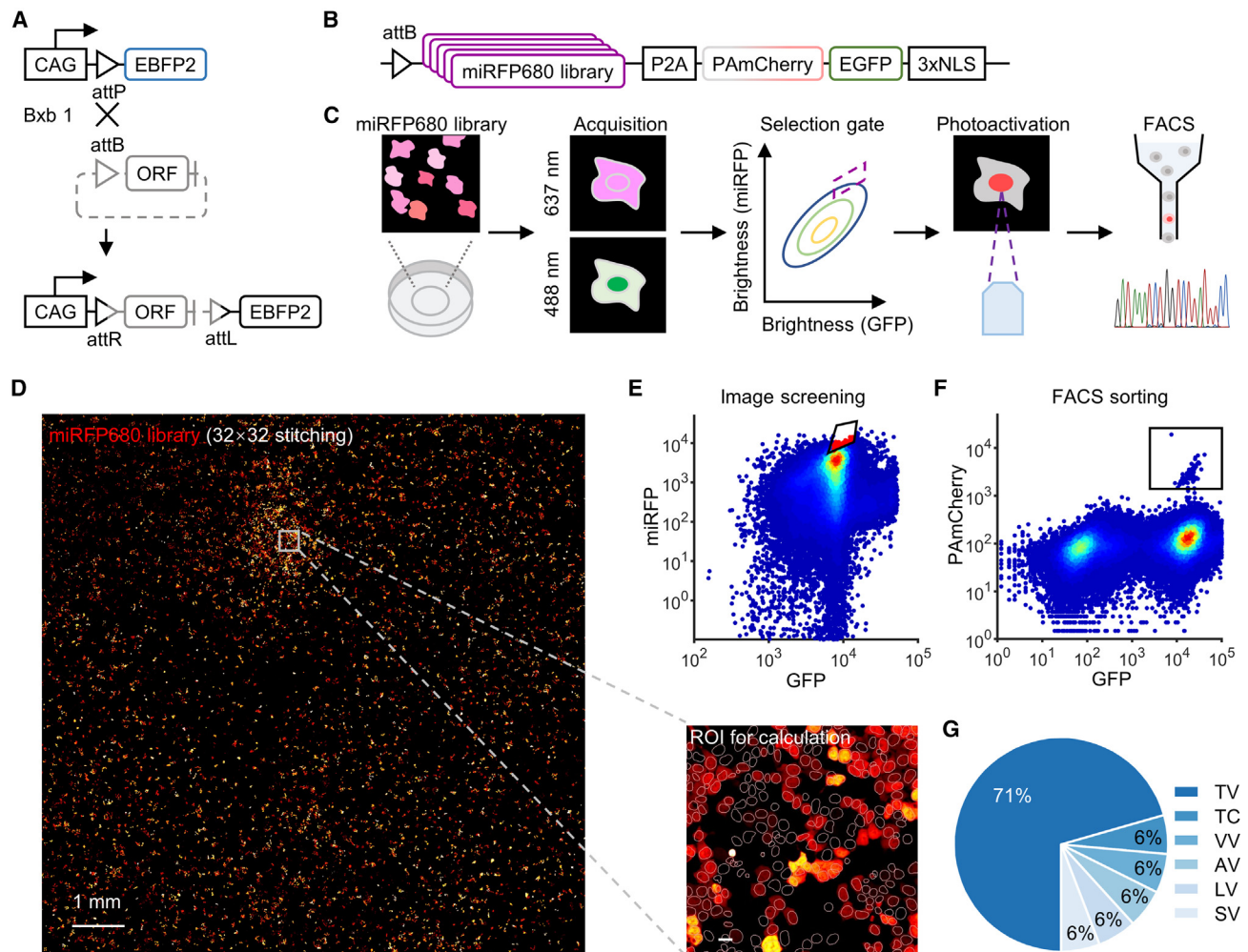
Figure 2. Construction and screening of miRFP680 library

(A) Scheme of gene integration in CAG-LLP cell line. ORF, open reading frame.

(B) Construction of miRFP680 library.

(C) Pipeline of screening of fluorescent protein by Faculae.

(D) The stitching image and segmented regions of interest (ROIs) of the cell library expressing miRFP680 mutants. The regions of nuclear localized EGFP in each cell were clearly identified.

(E) Cells with relatively high miRFP brightness were photoactivated under microscope (red scatters in black gate).

(F) PAmCherry$^+$ cells were recovered by FACS (black gate).

(G) The proportion of sequencing results of retrieved PAmCherry$^+$ cells. The double letters represented residues 202 and 203, e.g., "TV" represents T202, V203. See also Figure S2 and Table S2.

were successfully PCR amplified for Sanger sequencing. 12 out of 17 (71%) of the sequencing results converged to miRFP680 (202T/203V) (Figure 2G; Table S2). We further confirmed that miRFP680 is the brightest candidate in the recovered mutants (Figure S2E). Together, the above experiments demonstrated that Faculae could enrich mutants exhibiting desired phenotypes in the image-based screening from a pooled library.

Multidimensional imaging-guided screening of improved FR calcium sensor

We next applied Faculae to improve the performance of NIR-GECO (Figure 3A). First, to evaluate both the baseline brightness

(F_0) and the SBR ($\Delta F/F_0$) of the mutants within each cell, we sought to manipulate the intracellular calcium concentration through drug treatment (Figure 3B). Our initial attempt at using a combination of ionomycin and $CaCl_2$ in HEK 293T cells failed, as the calcium concentration oscillates rather than reaching a steady state (Figure S3A). To inhibit the fluctuations, we added 2-APB to the imaging buffer to block gap junction and store-operated Ca^{2+} entry,[27,28] which resulted in steady calcium levels (Figure S3B). We applied this ionomycin/$CaCl_2$/2-APB treatment protocol to compare the SBR of GCaMP6s with GCaMP5g, which were readily resolved (Figures S3C–S3E). We then utilized this strategy to compare the SBRs of NIR-GECO2G
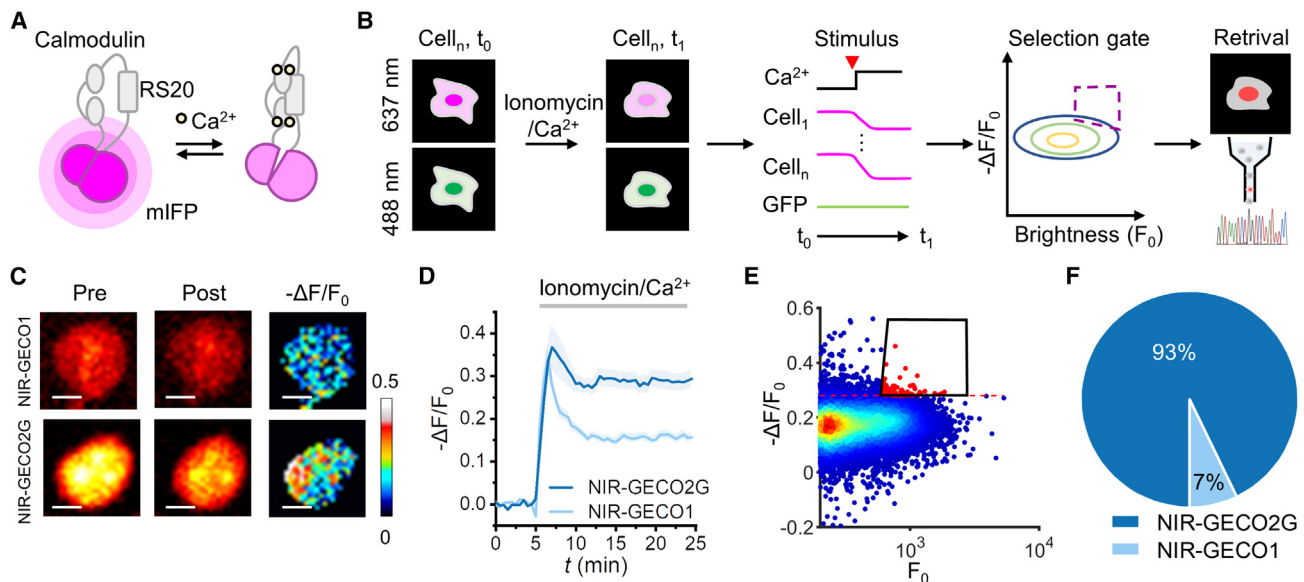
Figure 3. A multiparametric strategy for NIR-GECO evaluation

(A) Schematic representation of NIR-GECO.

(B) Workflow of NIR-GECO screening by Faculae.

(C) Example images of HEK 293T cells expressing the indicated nuclear targeted NIR-GECOs. The fluorescence response in the presence of 2 μM ionomycin and 1 mM CaCl$_2$ is shown.

(D) The response traces of NIR-GECOs in the presence of 2 μM ionomycin and 1 mM CaCl$_2$. Shadow areas represent SEM. n_{cell} = 9 for NIR-GECO2G; n_{cell} = 9 for NIR-GECO1.

(E) Cells with relatively high brightness and large SBR were photoactivated under microscope (red scatters in black gate). Red dashed line represents $-\Delta F/F_0$ = 0.28, the average SBR of NIR-GECO2G.

(F) The proportion of sequencing results of retrieved PAmCherry$^+$ cells. 50 μM 2-APB was present throughout imaging.

See also Figure S3.

and NIR-GECO1. Time-lapse imaging showed that NIR-GECO2G had higher SBR ($\Delta F/F_0$ = −28% ± 2%) than NIR-GECO1 ($\Delta F/F_0$ = −15% ± 1%) (Figures 3C and 3D), which was consistent with the previous report,[17] thus demonstrating the general applicability of our approach.

Next, we performed a model screen by mixing cells expressing either NIR-GECO2G or NIR-GECO1 with a ratio of 1–20. To improve the precision of measurement and to minimize the effect of cell movement, we localized NIR-GECOs and superfolder GFP[29] (sfGFP) to the nucleus. The calcium-insensitive sfGFP could serve as an expression reference and a marker for motion correction[30] (Figure 3B). We reduced cell migration by optimizing the coating material in the culture dish prior to seeding cells and starving cells from serum for 16–20 h prior to the measurement (Figure S3F). We screened over 5 × 10^4 cells and photoactivated 85 cells (0.2%) with relatively high brightness and large fluorescence change for FACS (Figure 3E; Table S2). Notably, despite taking up merely 5% in the initial pool, NIR-GECO2G constitutes 93% of sequencing results (Figure 3F), indicating that Faculae had the potential to enrich high-performance candidates in a pooled biosensor library.

We created several combinational mutagenesis libraries starting from NIR-GECO2G.[17] First, we constructed two libraries targeting the mIFP domain and the CaM-RS20 domain, respectively (Figures 4A and 4B). In each library, 17 sites based on previously

reported mutations in GECIs were targeted for random codon mutagenesis.[30–35] Plasmid libraries with an average of ~2 targeted codon mutations per gene were generated by previously reported methods[36] (Figure S4A). To increase the copy number of high-performance mutants, we enriched cells with high basal fluorescence by FACS and cultured them until screening (Figures S4B and S4C). Based on the screening results of these two libraries, we picked V133 and S466 from the mIFP library and N302 from the CaM library as high-mutation-rate residues for further saturated combinational mutagenesis (Figures 4A, 4B, and S4D–S4F). In the previous research, these three sites were mutated in the evolution for NIR-GECO1.[18] We analyzed ~1 × 10^5 cells carrying ~8,000 possible combinations. Compared with the first two libraries, the combined library had clearly shifted to higher F_0 and $\Delta F/F_0$ (Figures 4C and 4D). Meanwhile, different from previous libraries, the sequencing results from the combined library revealed completely no template, suggesting that these selected mutants were promising targets with better performance (Figure 4E). Since no dominant mutants were observed (Figure 4F), we evaluated all of them by measuring their brightness and response to ionomycin/CaCl$_2$/2-APB treatment in HEK 293T cells (Figures 4G and S4G). The fold change in basal brightness of these mutants ranged from 1.3 ± 0.1 (mean ± SEM, same below; NIR-GECO2G-133S/302T/466M, abbreviated as STM) to 3.4 ± 0.1 (NIR-GECO2G-133D/302Q/466V,
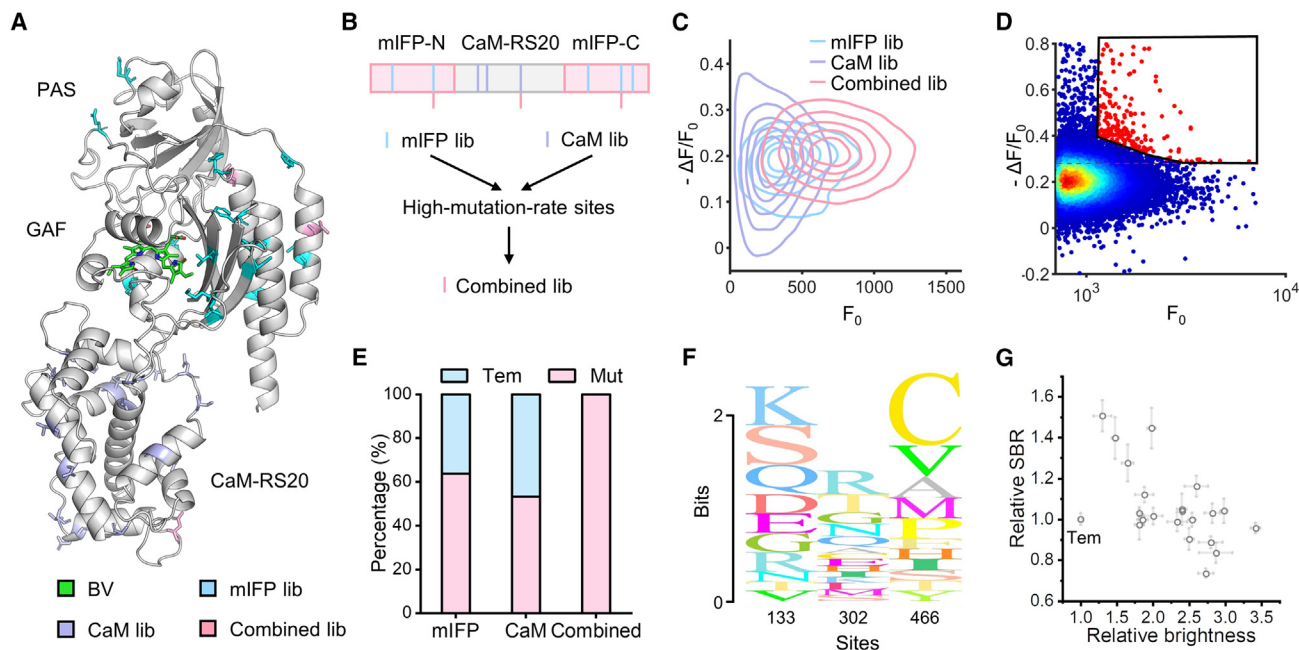
Figure 4. Evolving NIR-GECO2G by Faculae

(A) Predicted structure of NIR-GECO2G (predicted on Uni-Fold[37]). The chromophore and mutation sites are highlighted.

(B) Design of the mutagenesis sites in indicated libraries.

(C) The screening contour of three libraries. In each library, the contour lines from center to periphery represent relative estimated density from 83% to 17%.

(D) In combined library, cells with relatively high brightness and SBR were photoactivated under microscope (red scatters in black gate).

(E) The proportion of template (NIR-GECO2G) and mutants in sequencing results.

(F) Sequence logo of the screening result in the combined library.

(G) Characterization of SBR and brightness for each mutant in HEK 293T. For SBR tests, at least eight cells of one mutant were calculated. For brightness tests, at least three replicates were analyzed by flow cytometry. Error bars represent SEM.

See also Figure S4 and Table S3.

---

abbreviated as DQV), and the fold change in SBR ranged from 0.73 ± 0.02 (NIR-GECO2G-133R/302Q/466P, abbreviated as RQP) to 1.5 ± 0.1 (STM), compared with the template. All of the mutants showed increased brightness. Among these, five mutants exhibited significantly improved SBR (Table S3). We also confirmed that the photostability of most variants was not compromised (Figure S4H; Table S3).

We selected several candidates with improved properties and evaluated their response to physiological signals in rat cultured hippocampal neurons (Table S4). We performed whole-cell patch clamp and stimulated action potential firing via injecting current pulses of 300 pA for 10 ms. We measured the fluorescent response to 1–10 action potentials (50 Hz pulses) and quantified kinetic parameters including half-rise time and half-decay time. We identified two NIR-GECO2G mutants with better performance than the template: 133Q/302K/466M (named Nier1s) and 133E/302T/466C (named Nier1b). Both Nier1s and Nier1b are uniformly distributed in the neuronal cytoplasm (Figure 5A). Compared to the template, Nier1s exhibited similar brightness (1.2- $\pm$ 0.2-fold) and enhanced action potential response ($-5.8\% \pm 0.9\%$ versus $2.9\% \pm 0.5\%$ for single action potential), while Nier1b showed improved brightness (1.9- $\pm$ 0.2-fold) and similar fluorescence change ($-3\% \pm 0.6\%$ for single action potential) (Figures 5B–5E, S5A, and S5B; Table S4). Both indicators showed better signal-

to-noise ratio (SNR) than the template with similar response kinetics (Figures 5F–5H). We next characterized FR-GECIs *in vitro*. Nier1s and Nier1b had similar absorption and emission peaks, pKa values, and Hill coefficients (Figures S5C–S5J; Table S5). Compared to NIR-GECO2G, Nier1s has similar molecular brightness (defined as the product of extinction coefficient and quantum yield) and 2-fold higher dynamic range ($F_{max}/F_{min} = 24$ versus 12), while Nier1b has 1.6-fold higher molecular brightness but lower dynamic range ($F_{max}/F_{min} = 4.5$ versus 12). The K_d values of Nier1s (146 nM) and Nier1b (308 nM) are comparable to that of NIR-GECO2G (194 nM).

We performed another round of evolution from Nier1s to demonstrate the efficiency and convenience of Faculae. We constructed a randomly mutated library of 14 sites based on previously reported mutations in iBB-GECO1, an FR calcium indicator engineered from NIR-GECO2.[38] In the first round of enrichment, we photoselected 1,986 cells within 50 min and retrieved 800 cells from FACS, which were amplified for the next round of iterative library construction (Figure 6A). In the second round of enrichment, we observed a substantial increase in the average brightness (2.1×10^2 versus 4.4×10^2), with few changes in the average fluorescence response (-26.2% versus -26.0%) of the cell population (Figure 6B). We sequenced individual cells following the same procedure
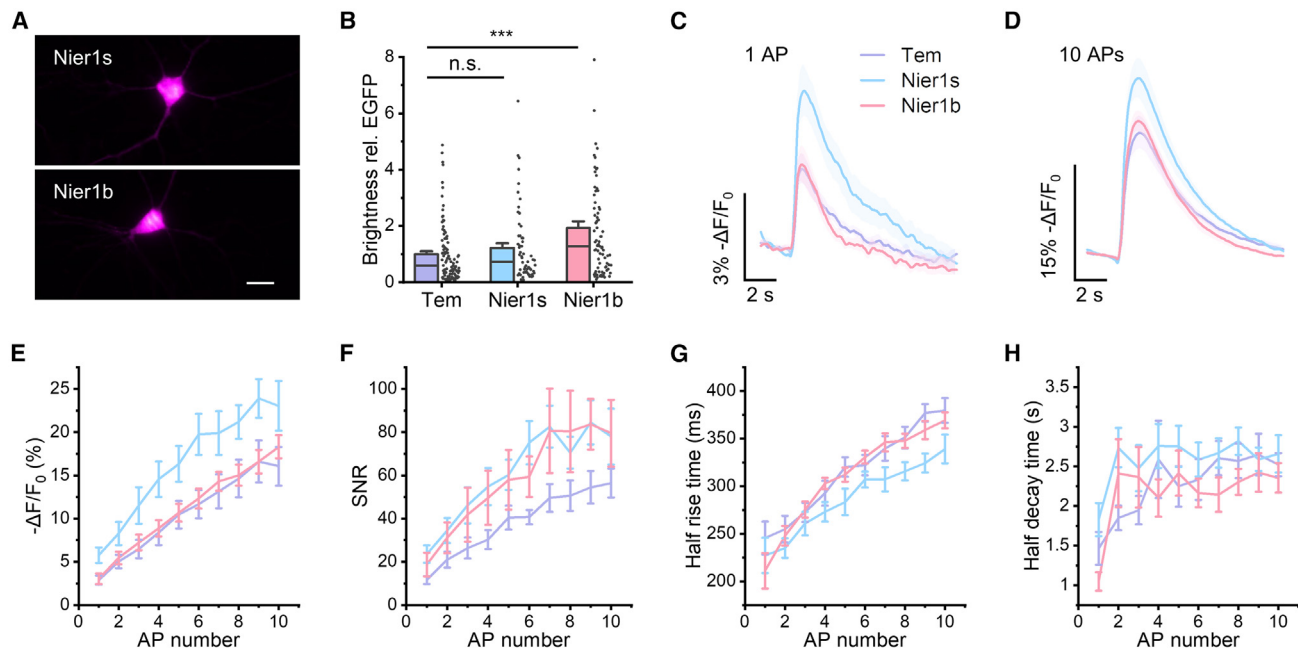
Figure 5. Nier performance in cultured neurons

(A) Representative images of Nier1s and Nier1b. Scale bar: 20 μm.

(B) Brightness of Nier1s (64 cells) and Nier1b (79 cells) normalized to NIR-GECO2G (105 cells). Cells were imaged at days *in vitro* (DIV) 16–18 with no supply of exogenous BV. ***p < 0.001 (Mann-Whitney test).

(C) Averaged responses to 1 action potential (AP) for NIR-GECO2G, Nier1s and Nier1b. Shaded areas represent SEM.

(D) Averaged responses to 10 APs for NIR-GECO2G, Nier1s, and Nier1b. Shaded areas represent SEM.

(E–H) Measured fluorescence change (E), SNR at 48 Hz imaging rate (F), half-rise time (G), and half-decay time (H) as functions of AP numbers. Error bars represent SEM.

(C–H) n_{cell} = 10 for NIR-GECO2G; n_{cell} = 10 for Nier1s; n_{cell} = 10 for Nier1b.

See also Figure S5 and Table S4.

as in the evolution of Nier1s and found that 8 out of 21 clones were Nier1s, while 7 clones contained 323ΔGG deletion (Figure S6). We evaluated Nier1s-323ΔGG and other mutants in HEK 293T cells (Figure 6C; Table S6). Nier1s-323ΔGG has lower brightness (0.82 ± 0.04) despite its higher SBR (1.06 ± 0.05) compared with Nier1s. Unexpectedly, Nier1s-S373Y and Nier1s-Y271F/l378C showed increased baseline brightness (1.54 ± 0.07; 1.24 ± 0.09) and $\Delta F/F_0$ (1.15 ± 0.02; 1.10 ± 0.03). These results demonstrate that Faculae is fast and convenient for iterative evolution.

DISCUSSION

We developed Faculae, a functional imaging-guided cell selection strategy for engineering genetically encoded fluorescent indicators. We achieved multiparametric screen of 0.4–1 × 10^5 cells within 1.5 h and photoactivation of ~2 × 10^3 cells within 50 min. Faculae has several advantages. In terms of screening throughput per round, it is on par with Photopick (0.6–1 × 10^5) and outperforms Opto-MASS (0.1–0.2 × 10^5) by several fold. Faculae also enables fast photoselection of target cells, with 1–1.5 s spot illumination per cell, which compares favorably against the aspiration-based approach in Opto-MASS (typically requiring 1–2 min per cell).

Faculae and Photopick share a conceptually similar phototagging mechanism but differ in one key aspect: while Photopick uses DMD-based wide-field illumination to photoconvert multiple cells in parallel at a low power density (0.04 W/cm²), Faculae applies spot illumination to photoconvert individual cells one at a time with a high power density (80 W/cm²). Faculae is thus more efficient than Photopick when only a few cells (<2 × 10^3) need to be retrieved. If one expects to collect a large population of cells from the pool, the Photopick approach would be more suitable.

Faculae has enabled the measurement of tens of thousands of mutants, allowing us to rapidly improve the brightness and SBR of FR-GECIs. We envision that Faculae has extensive applications for sensor engineering. It is compatible with biosensors of various spectra, including green, red, FR, and near-infrared, because both PA-GFP and PAmCherry can provide a high photoactivation contrast ratio for FACS. The CAG-LLP HEK 293T line ensures strong expression of target proteins, making Faculae suitable for unoptimized biosensors with low fluorescent intensity.

In addition to brightness and SBR, Faculae can in principle be leveraged to assess many other properties of biosensors. For example, the photostability of fluorescent indicators can be tested by photobleaching illumination, while the substrate affinity can be assayed by dosing treatment, as previously reported.[11,39]
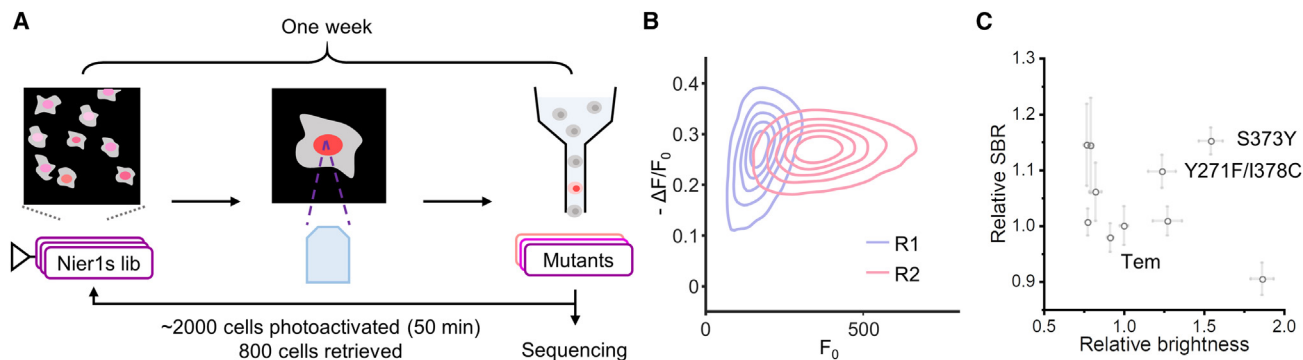
Figure 6. Iterative evolution by Faculae
(A) Pipeline for Faculae-based iterative evolution starting from Nier1s.
(B) The screening contour of the libraries in two rounds. In each library, the contour lines from center to periphery represent relative estimated density from 83% to 17%.
(C) Characterization of the SBR (n ≥ 10 cells per mutant) and brightness (n ≥ 2 replicates) for each mutant in HEK 293T cells. Error bars represent SEM.
See also Figure S6 and Table S6.

Furthermore, subcellular protein distribution and its dynamic changes could also be readily monitored due to the high spatio-temporal resolution of fluorescence imaging.[9,13] Since Faculae is performed in mammalian cells, it would be particularly useful for the directed evolution of membrane proteins, such as indicators based on G protein-coupled receptors and rhodopsins,[1,3] which has proven difficult for bacterial screens. Similarly, Faculae would be valuable for engineering tools that are designed to perturb the mammalian systems, such as chemogenetic tools and optogenetic tools,[40,41] or those that rely on complex mammalian pathways, such as biosensors for kinase activity.[42]

The FR-GECIs, namely Nier1s and Nier1b, showed improved SBR and brightness compared to template, emphasizing the importance of large-scale multiparameter screens in mammalian cells. During directed evolution for NIR-GECO1, the three key mutations D133V, I302N, and F466S were introduced to the sensor scaffold.[18] However, our screening experiments identified better combinations (e.g., NIR-GECO2G-133Q/302K/466M for Nier1s and NIR-GECO2G-133E/302T/466C for Nier1b) on these sites, resulting in better FR-GECIs for recording neural activity. Although array-based screening of FR-GECI mutants in bacterial lysate in the original studies achieved multidimensional characterization, it was still limited by screening throughput and did not match the intended mammalian environment, which might lead to suboptimal mutations.[43]

The gene recovery efficiency of Faculae depends on the FACS retrieval yield and the success of single-cell PCR, both of which are imperfect. The average FACS retrieval yield is 44% ± 8% (mean ± SD, 2 trials), which is close to a previously reported yield of 54%.[11] The PCR recovery rate varies from 24% to 51%. We speculate that the single copy of the gene in the LLP cell line causes the low recovery rate, making it difficult to amplify the mutant gene. We can compensate for the gene information loss by increasing the redundancy of mutants in the initial cell library.

As an image-based directed evolution methodology in mammalian system, Faculae can be further optimized on the following aspects: library construction and phenotyping.[44,45]

First, the library scale can be increased by incorporating newly developed recombinase into the LLP technique.[46] Second, the phenotyping throughput can be further improved by applying large field-of-view setups and advanced cell detection approaches[47,48] so that we can derive complex phenotypic information from a greater number of cells. Overall, we anticipate that Faculae will become a generalizable method for biomolecular engineering.

Limitations of the study
Faculae is a pooled screening platform based on imaging. While it can measure both static and dynamic parameters such as brightness and SBR across multiple fields of view, it is not suited for measuring kinetic parameters such as fluorescence response time constants. Faculae also relies on FACS for sorting tagged cells, which requires that drug treatment during the imaging session should not damage cells.

STAR★METHODS

Detailed methods are provided in the online version of this paper and include the following:

- KEY RESOURCES TABLE
- RESOURCE AVAILABILITY
  - Lead contact
  - Materials availability
  - Data and code availability
- EXPERIMENTAL MODEL AND SUBJECT DETAILS
  - Cultured cell models
- METHOD DETAILS
  - Molecular cloning
  - Cell transfection
  - Library construction
  - Stable cell line construction
  - Imaging apparatus and confocal microscopy
  - Time-lapse imaging
  - Imaging-based screening

Cell Reports Methods
Article

- ○ Flow cytometry
- ○ Electrophysiology
- ○ Brightness and photobleaching test
- ○ Protein purification and *in vitro* characterization
- ○ Wide-field calcium imaging in rat hippocampal neuron culture
- ● QUANTIFICATION AND STATISTICAL ANALYSIS

REFERENCES

1. Sabatini, B.L., and Tian, L. (2020). Imaging neurotransmitter and neuromodulator dynamics *in vivo* with genetically encoded indicators. Neuron *108*, 17–32. https://doi.org/10.1016/j.neuron.2020.09.036.

2. Inoue, M. (2021). Genetically encoded calcium indicators to probe complex brain circuit dynamics in vivo. Neurosci. Res. *169*, 2–8. https://doi.org/10.1016/j.neures.2020.05.013.

3. Xu, Y., Zou, P., and Cohen, A.E. (2017). Voltage imaging with genetically encoded indicators. Curr. Opin. Chem. Biol. *39*, 1–10. https://doi.org/10.1016/j.cbpa.2017.04.005.

4. Babakhanova, S., Jung, E.E., Namikawa, K., Zhang, H., Wang, Y., Subach, O.M., Korzhenevskiy, D.A., Rakitina, T.V., Xiao, X., Wang, W., et al. (2022). Rapid directed molecular evolution of fluorescent proteins in mammalian cells. Protein Sci. *31*, 728–751. https://doi.org/10.1002/pro.4261.

5. Villette, V., Chavarha, M., Dimov, I.K., Bradley, J., Pradhan, L., Mathieu, B., Evans, S.W., Chamberland, S., Shi, D., Yang, R., et al. (2019). Ultrafast two-photon imaging of a high-gain voltage indicator in awake behaving

6. Dong, A., He, K., Dudok, B., Farrell, J.S., Guan, W., Liput, D.J., Puhl, H.L., Cai, R., Wang, H., Duan, J., et al. (2022). A fluorescent sensor for spatiotemporally resolved imaging of endocannabinoid dynamics in vivo. Nat. Biotechnol. *40*, 787–798. https://doi.org/10.1038/s41587-021-01074-4.

7. Wardill, T.J., Chen, T.W., Schreiter, E.R., Hasseman, J.P., Tsegaye, G., Fosque, B.F., Behnam, R., Shields, B.C., Ramirez, M., Kimmel, B.E., et al. (2013). A neuron-based screening platform for optimizing genetically-encoded calcium indicators. PLoS One *8*, e77728. https://doi.org/10.1371/journal.pone.0077728.

8. Kanfer, G., Sarraf, S.A., Maman, Y., Baldwin, H., Dominguez-Martin, E., Johnson, K.R., Ward, M.E., Kampmann, M., Lippincott-Schwartz, J., and Youle, R.J. (2021). Image-based pooled whole-genome CRISPRi screening for subcellular phenotypes. J. Cell Biol. *220*, e202006180. https://doi.org/10.1083/jcb.202006180.

9. Yan, X., Stuurman, N., Ribeiro, S.A., Tanenbaum, M.E., Horlbeck, M.A., Liem, C.R., Jost, M., Weissman, J.S., and Vale, R.D. (2021). High-content imaging-based pooled CRISPR screens in mammalian cells. J. Cell Biol. *220*, e202008158. https://doi.org/10.1083/jcb.202008158.

10. Hasle, N., Cooke, A., Srivatsan, S., Huang, H., Stephany, J.J., Krieger, Z., Jackson, D., Tang, W., Pendyala, S., Monnat, R.J., Jr., et al. (2020). High-throughput, microscope-based sorting to dissect cellular heterogeneity. Mol. Syst. Biol. *16*, e9442. https://doi.org/10.15252/msb.20209442.

11. Lee, J., Liu, Z., Suzuki, P.H., Ahrens, J.F., Lai, S., Lu, X., Guan, S., and St-Pierre, F. (2020). Versatile phenotype-activated cell sorting. Sci. Adv. *6*, eabb7438. https://doi.org/10.1126/sciadv.abb7438.

12. Chien, M.-P., Brinks, D., Testa-Silva, G., Tian, H., Phil Brooks, F., Adam, Y., Bloxham, B., Gmeiner, B., Kheifets, S., and Cohen, A.E. (2021). Photoactivated voltage imaging in tissue with an archaerhodopsin-derived reporter. Sci. Adv. *7*, eabe3216. https://doi.org/10.1126/sciadv.abe3216.

13. Kudo, T., Lane, K., and Covert, M.W. (2022). A multiplexed epitope barcoding strategy that enables dynamic cellular phenotypic screens. Cell Syst. *13*, 376–387.e8. https://doi.org/10.1016/j.cels.2022.02.006.

14. Tian, H., Davis, H.C., Wong-Campos, J.D., Park, P., Fan, L.Z., Gmeiner, B., Begum, S., Werley, C.A., Borja, G.B., Upadhyay, H., et al. (2023). Video-based pooled screening yields improved far-red genetically encoded voltage indicators. Nat. Methods, 2023/01/09. https://doi.org/10.1038/s41592-022-01743-5.

15. Rappleye, M., Gordon-Fennel, A., Castro, D.C., Matarasso, A.K., Zamorano, C.A., Stine, C., Wait, S.J., Lee, J.D., Siebart, J.D., Suko, A., et al. (2022). Opto-MASS: a high-throughput engineering platform for genetically encoded fluorescent sensors enabling all optical in vivo detection of monoamines and neuropeptides. bioRxiv494241. https://doi.org/10.1101/2022.06.01.494241.

16. Shemetov, A.A., Monakhov, M.V., Zhang, Q., Canton-Josh, J.E., Kumar, M., Chen, M., Matlashov, M.E., Li, X., Yang, W., Nie, L., et al. (2021). A near-infrared genetically encoded calcium indicator for in vivo imaging. Nat. Biotechnol. *39*, 368–377. https://doi.org/10.1038/s41587-020-0710-1.

17. Qian, Y., Cosio, D.M.O., Piatkevich, K.D., Aufmkolk, S., Su, W.C., Celiker, O.T., Schohl, A., Murdock, M.H., Aggarwal, A., Chang, Y.-F., et al. (2020). Improved genetically encoded near-infrared fluorescent calcium ion indicators for in vivo imaging. PLoS Biol. *18*, e3000965. https://doi.org/10.1371/journal.pbio.3000965.

18. Qian, Y., Piatkevich, K.D., Mc Larney, B., Abdelfattah, A.S., Mehta, S., Murdock, M.H., Gottschalk, S., Molina, R.S., Zhang, W., Chen, Y., et al. (2019). A genetically encoded near-infrared fluorescent calcium ion indicator. Nat. Methods *16*, 171–174. https://doi.org/10.1038/s41592-018-0294-6.

19. Victora, G.D., Schwickert, T.A., Fooksman, D.R., Kamphorst, A.O., Meyer-Hermann, M., Dustin, M.L., and Nussenzweig, M.C. (2010). Germinal

mice. Cell *179*, 1590–1608.e23. https://doi.org/10.1016/j.cell.2019.11.004.

Center Dynamics Revealed by Multiphoton Microscopy with a Photoactivatable Fluorescent Reporter. Cell *143*, 592–605. https://doi.org/10.1016/j.cell.2010.10.032.

20. Tomura, M., Yoshida, N., Tanaka, J., Karasawa, S., Miwa, Y., Miyawaki, A., and Kanagawa, O. (2008). Monitoring cellular movement in vivo with photoconvertible fluorescence protein "Kaede" transgenic mice. Proc. Natl. Acad. Sci. USA *105*, 10871–10876. https://doi.org/10.1073/pnas.0802278105.

21. Medaglia, C., Giladi, A., Stoler-Barak, L., De Giovanni, M., Salame, T.M., Biram, A., David, E., Li, H., Iannacone, M., Shulman, Z., and Amit, I. (2017). Spatial reconstruction of immune niches by combining photoactivatable reporters and scRNA-seq. Science *358*, 1622–1626. https://doi.org/10.1126/science.aao4277.

22. Callaway, E.M., and Katz, L.C. (1993). Photostimulation using caged glutamate reveals functional circuitry in living brain slices. Proc. Natl. Acad. Sci. USA *90*, 7661–7665. https://doi.org/10.1073/pnas.90.16.7661.

23. Subach, F.V., Patterson, G.H., Manley, S., Gillette, J.M., Lippincott-Schwartz, J., and Verkhusha, V.V. (2009). Photoactivatable mCherry for high-resolution two-color fluorescence microscopy. Nat. Methods *6*, 153–159. https://doi.org/10.1038/nmeth.1298.

24. Patterson, G.H., and Lippincott-Schwartz, J. (2002). A photoactivatable GFP for selective photolabeling of proteins and cells. Science *297*, 1873–1877. https://doi.org/10.1126/science.1074952.

25. Matreyek, K.A., Stephany, J.J., Chiasson, M.A., Hasle, N., and Fowler, D.M. (2020). An improved platform for functional assessment of large protein libraries in mammalian cells. Nucleic Acids Res. *48*, e1. https://doi.org/10.1093/nar/gkz910.

26. Matlashov, M.E., Shcherbakova, D.M., Alvelid, J., Baloban, M., Pennacchietti, F., Shemetov, A.A., Testa, I., and Verkhusha, V.V. (2020). A set of monomeric near-infrared fluorescent proteins for multicolor imaging across scales. Nat. Commun. *11*, 239. https://doi.org/10.1038/s41467-019-13897-6.

27. Bai, D., del Corsso, C., Srinivas, M., and Spray, D.C. (2006). Block of specific gap junction channel subtypes by 2-aminoethoxydiphenyl borate (2-APB). J. Pharmacol. Exp. Therapeut. *319*, 1452–1458. https://doi.org/10.1124/jpet.106.112045.

28. Bootman, M.D., Collins, T.J., Mackenzie, L., Roderick, H.L., Berridge, M.J., and Peppiatt, C.M. (2002). 2-aminoethoxydiphenyl borate (2-APB) is a reliable blocker of store-operated Ca^{2+} entry but an inconsistent inhibitor of InsP3-induced Ca^{2+} release. Faseb. J. *16*, 1145–1150. https://doi.org/10.1096/fj.02-0037rev.

29. Pédelacq, J.D., Cabantous, S., Tran, T., Terwilliger, T.C., and Waldo, G.S. (2006). Engineering and characterization of a superfolder green fluorescent protein. Nat. Biotechnol. *24*, 79–88. https://doi.org/10.1038/nbt1172.

30. Subach, O.M., Barykina, N.V., Anokhin, K.V., Piatkevich, K.D., and Subach, F.V. (2019). Near-infrared genetically encoded positive calcium indicator based on GAF-FP bacterial phytochrome. Int. J. Mol. Sci. *20*, 3488. https://doi.org/10.3390/ijms20143488.

31. Subach, O.M., and Subach, F.V. (2020). GAF-CaMP3-sfGFP, An Enhanced Version of the Near-Infrared Genetically Encoded Positive Phytochrome-Based Calcium Indicator for the Visualization of Neuronal Activity. Int. J. Mol. Sci. *21*, 6883. https://doi.org/10.3390/ijms21186883.

32. Zhao, Y., Araki, S., Wu, J., Teramoto, T., Chang, Y.-F., Nakano, M., Abdelfattah, A.S., Fujiwara, M., Ishihara, T., Nagai, T., and Campbell, R.E. (2011). An expanded palette of genetically encoded Ca^{2+} indicators. Science *333*, 1888–1891. https://doi.org/10.1126/science.1208592.

33. Chen, T.W., Wardill, T.J., Sun, Y., Pulver, S.R., Renninger, S.L., Baohan, A., Schreiter, E.R., Kerr, R.A., Orger, M.B., Jayaraman, V., et al. (2013). Ultrasensitive fluorescent proteins for imaging neuronal activity. Nature *499*, 295–300. https://doi.org/10.1038/nature12354.

34. Dana, H., Sun, Y., Mohar, B., Hulse, B.K., Kerlin, A.M., Hasseman, J.P., Tsegaye, G., Tsang, A., Wong, A., Patel, R., et al. (2019). High-performance calcium sensors for imaging activity in neuronal populations and microcompartments. Nat. Methods *16*, 649–657. https://doi.org/10.1038/s41592-019-0435-6.

35. Zarowny, L., Aggarwal, A., Rutten, V.M.S., Kolb, I., GENIE Project; Patel, R., Huang, H.Y., Chang, Y-F., Phan, T., Kanyo, R., et al. (2020). Bright and High-Performance Genetically Encoded Ca^{2+} Indicator Based on mNeonGreen Fluorescent Protein. ACS Sens. *5*, 1959–1968. https://doi.org/10.1021/acssensors.0c00279.

36. Belsare, K.D., Andorfer, M.C., Cardenas, F.S., Chael, J.R., Park, H.J., and Lewis, J.C. (2017). A simple combinatorial codon mutagenesis method for targeted protein engineering. ACS Synth. Biol. *6*, 416–420. https://doi.org/10.1021/acssynbio.6b00297.

37. Li, Z., Liu, X., Chen, W., Shen, F., Bi, H., Ke, G., and Zhang, L. (2022). Uni-Fold: an open-source platform for developing protein folding models beyond AlphaFold. Preprint at bioRxiv, 2022.2008.2004.502811. https://doi.org/10.1101/2022.08.04.502811.

38. Hashizume, R., Fujii, H., Mehta, S., Ota, K., Qian, Y., Zhu, W., Drobizhev, M., Nasu, Y., Zhang, J., Bito, H., and Campbell, R.E. (2022). A genetically encoded far-red fluorescent calcium ion biosensor derived from a biliverdin-binding protein. Protein Sci. *31*, e4440. https://doi.org/10.1002/pro.4440.

39. Koveal, D., Rosen, P.C., Meyer, D.J., Díaz-García, C.M., Wang, Y., Cai, L.-H., Chou, P.J., Weitz, D.A., and Yellen, G. (2022). A high-throughput multiparameter screen for accelerated development and optimization of soluble genetically encoded fluorescent biosensors. Nat. Commun. *13*, 2919. https://doi.org/10.1038/s41467-022-30685-x.

40. Sternson, S.M., and Roth, B.L. (2014). Chemogenetic tools to interrogate brain functions. Annu. Rev. Neurosci. *37*, 387–407. https://doi.org/10.1146/annurev-neuro-071013-014048.

41. Tischer, D., and Weiner, O.D. (2014). Illuminating cell signalling with optogenetic tools. Nat. Rev. Mol. Cell Biol. *15*, 551–558. https://doi.org/10.1038/nrm3837.

42. Mehta, S., Zhang, Y., Roth, R.H., Zhang, J.F., Mo, A., Tenner, B., Huganir, R.L., and Zhang, J. (2018). Single-fluorophore biosensors for sensitive and multiplexed detection of signalling activities. Nat. Cell Biol. *20*, 1215–1225. https://doi.org/10.1038/s41556-018-0200-6.

43. Tian, L., Hires, S.A., Mao, T., Huber, D., Chiappe, M.E., Chalasani, S.H., Petreanu, L., Akerboom, J., McKinney, S.A., Schreiter, E.R., et al. (2009). Imaging neural activity in worms, flies and mice with improved GCaMP calcium indicators. Nat. Methods *6*, 875–881. https://doi.org/10.1038/nmeth.1398.

44. Lawson, M., and Elf, J. (2021). Imaging-based screens of pool-synthesized cell libraries. Nat. Methods *18*, 358–365. https://doi.org/10.1038/s41592-020-01053-8.

45. Hendel, S.J., and Shoulders, M.D. (2021). Directed evolution in mammalian cells. Nat. Methods *18*, 346–357. https://doi.org/10.1038/s41592-021-01090-x.

46. Durrant, M.G., Fanton, A., Tycko, J., Hinks, M., Chandrasekaran, S.S., Perry, N.T., Schaepe, J., Du, P.P., Lotfy, P., Bassik, M.C., et al. (2023). Systematic discovery of recombinases for efficient integration of large DNA sequences into the human genome. Nat. Biotechnol. *41*, 488–499. https://doi.org/10.1038/s41587-022-01494-w.

47. Werley, C.A., Chien, M.-P., and Cohen, A.E. (2017). Ultrawidefield microscope for high-speed fluorescence imaging and targeted optogenetic stimulation. Biomed. Opt Express *8*, 5794–5813. https://doi.org/10.1364/BOE.8.005794.

48. Pachitariu, M., and Stringer, C. (2022). Cellpose 2.0: how to train your own model. Nat. Methods *19*, 1634–1641. https://doi.org/10.1038/s41592-022-01663-4.

49. Edelstein, A.D., Tsuchida, M.A., Amodaj, N., Pinkard, H., Vale, R.D., and Stuurman, N. (2014). Advanced methods of microscope control using

μManager software. J. Biol. Methods *1*, e10. https://doi.org/10.14440/jbm.2014.36.

50. Liu, S., Lin, C., Xu, Y., Luo, H., Peng, L., Zeng, X., Zheng, H., Chen, P.R., and Zou, P. (2021). A far-red hybrid voltage indicator enabled by bio-orthogonal engineering of rhodopsin on live neurons. Nat. Chem. *13*, 472–479. https://doi.org/10.1038/s41557-021-00641-1.

51. Miyazaki, K. (2003). Creating random mutagenesis libraries by mega-primer PCR of whole plasmid (MEGAWHOP). In Directed Evolution Library Creation: Methods and Protocols, F.H. Arnold and G. Georgiou, eds. (Humana Press), pp. 22–28.

52. Schmidt, U., Weigert, M., Broaddus, C., and Myers, G. (2018). In Cell detection with star-convex polygons, A.F.F. Cham, J.A. Schnabel, C. Davatzikos, C. Alberola-López, and G. Fichtinger, eds. (Springer International Publishing), pp. 265–273, held in.

STAR★METHODS

KEY RESOURCES TABLE

REAGENT or RESOURCE	SOURCE	IDENTIFIER
Chemicals, peptides, and recombinant proteins		
Dulbecco's Modified Eagle's medium (DMEM)	Gibco	C11995500BT
Fetal Bovine Serum (FBS)	Gibco	100099044
Trypsin-EDTA (0.25%)	Gibco	25200056
Neurobasal™ Medium	Gibco	21103049
B-27™ Supplement	Gibco	17504044
GlutaMAX™ Supplement	Gibco	35050061
Penicillin-streptomycin	Beyotime	C0222
HBSS	Gibco	14025092
Blasticidin	Selleck	S7419
Matrigel® Matrix	Corning	356234
poly-D-lysine	Sigma	P7280-5X5M
Laminin Mouse Protein	Gibco	23017015
Opti-MEM® Medium	Gibco	31985062
Ionomycin	Cayman	11932
Protease K	Thermo	EO0491
HEPES	Amresco	0511
EGTA	Sigma	03777-10G
2-APB	Abcam	ab120124
Gabazine	Abcam	ab120042
NBQX	Abcam	ab120045
D-AP5 (APV)	Abcam	ab120003
Critical commercial assays		
Phanta® Max Super-Fidelity DNA Polymerase	Vazyme	P505-d2
ClonExpress II One Step Cloning Kit	Vazyme	C112-02
DNA extraction kit	TIANGEN	DP118-02
E.Z.N.A.® Gel Extraction kit	Omega	D2500
Ultra-Competent Cell Preps Kit	Sangon	B529303-0200
Lipofectamine® 2000 Reagent	Gibco	11668019
Lipofectamine® 3000 Reagent	Gibco	L3000008
Experimental models: Cell lines		
HEK 293T	ATCC	Cat#CRL-3216
Oligonucleotides		
Primers for mutation and single cell PCR, see Table S7	This paper	N/A
Recombinant DNA		
Plasmids for corresponding experiments, see Table S8	This paper	N/A
Software and algorithms		
FIJI/ImageJ	National Institutes of Health	Version 1.53t (https://imagej.net/Fiji)
MATLAB	The Mathworks, Inc., Natick, MA	R2018b (or later)
Micro-Manager	Arthur et al.[49]	2.0.0-gamma1
Custom code	This paper	See Method S1
LabVIEW	National Instruments Corp.	Version 2015

RESOURCE AVAILABILITY

Lead contact

Further information and requests for resources and reagents should be directed to and will be fulfilled by the lead contact, Dr. Peng Zou (zoupeng@pku.edu.cn).

Materials availability

Reagents in this study are available by request to lead contact, Dr. Peng Zou (zoupeng@pku.edu.cn).

Data and code availability

- All the data published in this paper will be available from the lead contact upon request.
- The MATLAB code is available as supporting information in this manuscript.
- Any additional information required to reanalyze the data reported in this paper is available from the lead contact upon request.

EXPERIMENTAL MODEL AND SUBJECT DETAILS

Cultured cell models

Human embryonic kidney 293T (HEK 293T) cells were incubated in Dulbecco's modified eagle medium (DMEM, Gibco) medium with 10% v/v fetal bovine serum (FBS, Gibco) at 37°C with 5% CO_2.

All experiments were done in accordance with the Experimental Animal Management Ordinance of Beijing, P. R. China. The protocol was approved by The Institutional Animal Care and Use Committee in Peking University. We did not select animal sex, and animals were housed in standard conditions. Primary rat hippocampal neurons were cultured as previous described.[50] Briefly, glass coverslips were incubated with 20 μg/mL poly-D-lysine (Sigma) solution and 10 μg/mL Laminin Mouse Protein (Gibco) solution for 24–48 h, respectively. Neurons were isolated from brains of neonatal Sprague-Dawley rat pups (postnatal day 0), and collected and diluted by neuronal culture medium (Neurobasal medium, B-27 supplement, GlutaMAX supplement and penicillin-streptomycin) to a final cell density of 6×10^4 cells/mL. 1 mL cell suspension was added to each 24-well containing pre-coated glass coverslip. Half of the neuron culture medium was replaced with fresh medium once every 4 days.

METHOD DETAILS

Molecular cloning

Plasmids were constructed using seamless cloning technique. The inserts and the vectors were PCR amplified (Vazyme, P505), gel purified (Omega, D2500) and then mixed with enzymes following manufacturer's instructions (Vazyme, C112). Successful clones were verified by Sanger sequencing. Site-directed mutagenesis and linker insertion/deletion were achieved by PCR overlap extension. The NIR-GECO1 gene and Bxb1 gene were synthesized by company. The descriptions of primers and plasmids used in this study are in Table S7 and Table S8. The plasmid maps are available from the corresponding authors upon request.

Cell transfection

HEK 293T cells were seeded in a 24-well plate and grown to 90% confluent for transfection. For each well, 500 ng plasmid and 1 μL Lipofectamine 2000 Reagent were mixed in Opti-MEM Medium and incubated for 5–10 min at room temperature. The mixture was added to the cell culture medium in the absence of serum for 4–8 h. Thereafter, cells were digested by Trypsin-EDTA (0.25%, Gibco), reseeded on a sterile 14-mm glass coverslip or a glass dish pre-treated with Matrigel Matrix, and incubated in the complete medium (DMEM+10%FBS) for 24–48 h before imaging.

Neurons were transfected on DIV7-9 (7–9 days *in vitro*). For each well, 500 ng plasmid DNA was mixed with 1.5 μL of Lipofectamine 3000 Reagent in the Neurobasal medium, before incubating with neurons for 45 min. The transfected neurons were imaged on DIV16-18.

Library construction

The NIR-GECO plasmid libraries (mIFP lib and CaM lib) were constructed via combinatorial codon mutagenesis[36] and MEGAWHOP method.[51] Mutations were introduced by designing oligonucleotide contain NNK triplet at the target sites. The upstream and downstream of primers contained 16 nucleotides for annealing (full length: 35 bp). The 17 forward-mutagenesis primers were mixed in equimolar quantities to generate the forward primer pool. The reverse primer pool was created by equally combined reverse complement of each of forward-mutagenesis primers (Table S7). The forward fragment PCR reaction contained 10 ng template, 1 μL forward primer pool (10 μM totally), 1 μL tail primer (10 μM), 12.5 μL 2×Phanta Max Buffer, 0.5 μL dNTP (10 mM each), 0.5 μL Phanta Max Super-Fidelity DNA Polymerase and 9 μL ddH₂O. The primer pair in reverse fragment PCR reaction was replaced by reverse primer pool and head primer. The forward and reverse reaction were used as templates for joining PCR without purification (1 μL each). The PCR program was set as below: 1) 95°C for 3 min; 2) 95°C for 15 s; 3) 50°C for 30 s, cooling to 50 °C at 0.5 °C/s; 4) 72°C for 60 s; 5)

Repeat steps 2 through 4 for 8 additional cycles if in fragment PCR, or 19 additional cycles if in joining PCR; 6) 72°C for 3 min; 7) Hold at 4°C. The PCR product was purified by gel extraction and used as the template for a second round of fragment-joining PCR step. The second-round PCR product was purified for MEGAWHOP. Mutations in combined lib were introduced by overlap extension PCR. The PCR product was purified for MEGAWHOP.

To create plasmid library from PCR products, 50 ng template attB plasmid (template) and 500–750 ng fragment (megaprimer) were mixed in 25 μL MEGAWHOP PCR reaction consisting of 12.5 μL 2×Phanta Max Buffer, 0.5 μL dNTP (10 mM each), 0.5 μL Phanta Max Super-Fidelity DNA Polymerase and ddH$_2$O. The PCR program was set as below: 1) 95°C for 3 min; 2) 95°C for 15 s; 3) 60°C for 15 s; 4) 72°C for 4 min; 5) Repeat steps 2 through 4 for 24 additional cycles; 6) 72°C for 3 min; 7) Hold at 4°C. The reaction was monitored by agarose gel electrophoresis as previously described.[51] The MEGAWHOP product was transferred into ultra-competent DH5α after DpnI treatment. Each 2 μL product was used to transform 1 tube of competent *E. coli* cells (100 μL). Transformation produced ∼1×10^5 constructs for 25 μL MEGAWHOP reaction. The competent cells were prepared using commercial kit based on rubidium chloride protocol (Sangon, B529303-0200). Plasmids were extracted from construct mixture (TIANGEN, DP118-02).

For cell library construction, CAG-LLP cells were seeded on a 6-cm dish to reach 90% confluence. Cells were transfected following Lipofectamine 3000 protocol (5.5 μg DNA, 11 μL P3000, 16 μL Lipofectamine 3000). After 6–8 h, cells were digested by trypsin and reseeded on a 10-cm dish. After 2 days, GFP$^+$/mIFP$^+$ cells were collected by FACS (∼200k) and expanded for at least 4 days. Then cells with strong GFP/mIFP signals were FACS enriched (∼100k) and seeded on a 35-mm glass dish. After 1 day, medium was changed to Opti-MEM Medium for reduced-serum cell culture, which could reduce cell movement during imaging. Cells were screened 1 day later. For miRFP680 screening and NIR-GECO screening test, cell libraries were produced and collected as described above but without expansion and FACS enrichment step.

Stable cell line construction

Lentivirus was produced in HEK293T cells. First, cells were seeded and grow to reach 90% confluence. Next, a DNA mix was prepared by combining expression plasmid, delta8.9 and VSVG at a mass ratio of 1:1:0.7 in Opti-MEM. The DNA was mixed with P3000 and then incubated with Lipofectamine 3000 at a ratio of 1:2:3 (w:v/v). Next, the above mix was added to cells and incubated at 37°C for 6–8 h. The old medium was aspirated and new complete medium was replenished. Cells were incubated for 40–48 h. The supernatant was collected and filtered through a 0.45-μm syringe. This lentivirus-contained medium was aliquoted and stored at −80°C.

For LLP cell line construction, HEK293T cells were infected with ∼0.1MOI when cell confluence reached 60%. After 48 h, cells were collected and sorted. BFP$^+$ single cells were seeded into a 96-well plate. Each well contain one clone in 150 μL complete medium. Cell clones grew at least 2 weeks before further validation. The desired clone was kept and expanded for following experiments. Cell culture medium was supplemented with 2.5 μg/mL Blasticidin (Selleck, S7419).

Imaging apparatus and confocal microscopy

All of the fluorescence imaging experiments were conducted on an inverted fluorescence microscope (Nikon-TiE) equipped with a 20 ×0.75 NA dry immersion objective lens (except for calcium imaging in neuron and photobleaching test, in which a 40× NA 1.3 oil immersion objective lens was used), four laser lines (Coherent OBIS 405 nm, 488 nm, 561 nm, and 637 nm), a spinning disk confocal unit (Yokogawa CSU-X1), and two scientific CMOS cameras (Hamamatsu ORCA-Flash 4.0 v2). The microscope, lasers, and cameras were controlled with either custom-built software written in LabVIEW (National Instruments, 15.0 version) or Micro-Manager 2.0 (MM2.0) and could switch between confocal and wide-field imaging modes. The spectra properties of filters and dichroic mirrors for various fluorescent indicators used in this study are summarized in Table S9. Image analysis was performed in ImageJ/Fiji (version 1.53t). ImageJ/Fiji and MM2.0 were run within MATLAB.

Time-lapse imaging

For ionomycin/CaCl$_2$/2-APB test, the transfected/recombined HEK293T cells were seeded on a 35-mm glass dish to reach 60–80% confluence. Cells were maintained in an extracellular (EC) Ca^{2+}-free medium containing 5 mM KCl, 135 mM NaCl, 1 mM MgCl$_2$, 0.4 mM KH$_2$PO$_4$, 10 mM glucose, and 20 mM HEPES (pH 7.4) at room temperature. Cells were incubated in EC with 50 μM 2-APB for at least 10 min before imaging. Time-lapse images were acquired with 20 s interval by LabVIEW. After 10 time points (∼200 s), the medium was replaced with EC containing 50 μM 2-APB, 2 μM Ionomycin and 1 mM CaCl$_2$ by peristaltic pump.

Imaging-based screening

For NIR-GECO screening, cells were incubated in EC with 50 μM 2-APB for at least 10 min before imaging. The first step was to acquire ∼500 2-channel images (330 μm × 330 μm each, defined as "pre-library" and "pre-marker") on a glass dish. Second, the buffer was replaced with EC containing 50 μM 2-APB, 2 μM Ionomycin and 1 mM CaCl$_2$. After 12 min, the second round of image acquisition of the same positions was performed ("post-library" and "post-marker"). All these images were processed through flat-filed correcting, including background subtraction. The post-marker images were segmented by StarDist.[52] ROIs were used to calculate nuclear sizes, intensities and xy coordinates. Brightness was defined as the maximum fluorescence (F$_{pre-library}$) of each cell. SBR was calculated as (F$_{post-library}$/F$_{post-marker}$ - F$_{pre-library}$/F$_{pre-marker}$)/(F$_{pre-library}$/F$_{pre-marker}$). For each library, 1.0–1.2×10^5 cells were screened in 1 or 2 dishes. Cells with both high brightness and large SBR (greater than the averaged values for the template) were manually gated. The positions of these cells were retrieved under microscope by moving the stage automatically. Cells were photoactivated one by one

for 1 s using focal illumination of 405 nm laser with 10% power (Coherent OBIS 405 nm, 50 mW). After photoactivation, the cells were maintained in EC containing 1 μM Ionomycin and 1 mM EGTA for 10 min. This step aimed to reduce intracellular concentration of calcium ion. Cells were digested, centrifuged and resuspended in PBS with 2% FBS. The cell suspension was kept on ice until FACS.

For miRFP680 screening, cells were incubated in HBSS for at least 10 min before imaging. the first step was to acquire 500–1000 2-channel images (defined as "library" and "marker") on a glass dish. All these images were processed through flat-filed correcting, including background subtraction. The marker images were segmented by StarDist. ROIs were used to calculate nuclear sizes, intensities and xy coordinates. Brightness was defined as the fluorescence ($F_{library}$ and F_{marker}) of each cell. Cells with high brightness were gated and photoactivated. After photoactivation, cells were digested, centrifuged and resuspended in HBSS with 2% FBS. The cell suspension was kept on ice until FACS.

For single cell nested PCR amplification, 96-well PCR plates were used to receive PAmCherry$^+$ single cells. Each well contained 5 μL PBS with 125 μg/mL Protease K. The plates were quickly frozen in liquid nitrogen after FACS. The lysates were treated in 56°C for 15 min and 95°C for 5 min. Next, 1 μL forward primer-1 (10 μM), 1 μL reverse primer-1 (10 μM), 12.5 μL 2×Phanta Max Buffer, 0.5 μL dNTP (10 mM each), 0.5 μL Phanta Max Super-Fidelity DNA Polymerase and 4.5 μL ddH$_2$O were added into the lysate in each well. After the first round of PCR, 3 μL reaction was used as template to perform the second round of PCR, while the primer pair was forward primer-2 and reverse primer-2. The PCR program was set as below: 1) 95°C for 3 min; 2) 95°C for 15 s; 3) 61°C for 15 s; 4) 72°C for 90 s; 5) Repeat steps 2 through 4 for 24 additional cycles if in first round PCR, or 34 additional cycles if in second round PCR; 6) 72°C for 3 min; 7) Hold 4°C. The PCR products were gel purified and verified by Sanger sequencing.

Flow cytometry

Cells were disassociated by trypsin and centrifuged at 300 g for 3 min. Cells were re-suspended in Hank's Balanced Salt Solution (HBSS, Gibco) containing 2% FBS and kept on ice until flow cytometry. Astrios EQ (BeckMan Coulter) was used for FACS sorting. The sorted cells were either lysed for PCR (see "Imaging-based screening" section) or cultured in DMEM with 10% FBS (see "Stable cell line construction" section). LSRFortessa was used for flow cytometry analysis (Becton Dickinson). Optical configuration of LSRFortessa: BFP (Ex: 405 nm, Em: 450/50), GFP (Ex: 488 nm, Em: 530/30), mCherry (Ex: 561 nm, Em: 610/20), miRFP680/mIFP (Ex: 640 nm, Em: 730/45).

Electrophysiology

For single-cell electrophysiology recording, cultured neurons were incubated in Tyrode's buffer containing 20 μM Gabazine, 10 μM NBQX and 25 μM APV. The electrophysiology experiments were performed at room temperature. Borosilicate glass electrodes (Sutter) were pulled to a tip resistance of 2.5–5 MΩ. The glass electrode was filled with internal solution containing 145 mM potassium gluconate, 5 mM MgCl$_2$, 10 mM HEPES, and 4 mM Na$_2$-ATP (pH 7.2, with KOH). The glass electrode's position was adjusted by a Sutter MP285 micro-manipulator. Membrane potentials were recorded under whole-cell current clamp under I = 0 mode (Axopatch 200B, Axon Instruments). Recorded membrane potential data were filtered with a 5 kHz internal Bessel filter in the amplified and digitized with a National Instruments PCIe-6353 data acquisition 1067 (DAQ) board. The microscope (Nikon Ti-E), the camera (Hamamatsu ORCA-Flash 4.0 v2) and electrophysiology recording system were controlled with a customized software written in LabVIEW 2015 (National Instruments), and the data were extracted and analyzed with a home-made script written in MATLAB R2018b (MathWorks).

Brightness and photobleaching test

HEK293T cells were transfected with pcDNA3.1-NIR-GECO-mut-3NLS-P2A-EGFP-3NLS using Lipofectamine 2000 Reagent as described in "Cell Culture and Transfection". For brightness test, cells were analyzed using flow cytometry. The brightness of each mutant was calculated as the median intensity of mIFP$^+$ cells. For photobleaching test, cells were continuously illuminated under microscope with 40× NA 1.3 objective. The power density of 637 nm laser was 9.0 W/cm^2.

Protein purification and *in vitro* characterization

The gene encoding Nier1s, Nier1b and NIR-GECO2G, with a polyhistidine tag on the N-terminus, was expressed from the pJC vector in E. coli strain BL21 (DE3). The bacteria were lysed with an ultrasonic cell disruptor and then centrifuged at 20000 rpm for 30 min. Extracted protein was purified by Ni-NTA agarose (QIAGEN). The eluted sample was dialyzed in PBS containing 1 mM DTT overnight. Proteins were further concentrated with an Amicon Ultra-15 Centrifugal Filter Device (Merck). The buffer was exchanged to 10 mM MOPS, 100 mM KCl (pH 7.2). We prepared a CaEGTA buffer (30 mM MOPS, 100 mM KCl, 10 mM EGTA, 10 mM CaCl$_2$) and an EGTA buffer (30 mM MOPS, 100 mM KCl, 10 mM EGTA).

Absorbance spectra of FR-GECIs were measured with NanoDrop 2000c (Thermo). Excitation and emission of FR-GECIs were measured with the Fluorescence Spectrophotometer F-7000 (HITACHI). For determination of the extinction coefficient, a ratio of maximum absorbance values of Q and Soret bands was calculated, assuming the latter to have the extinction coefficient of 39900 M^{-1} cm^{-1}. We used integrating sphere (FLS 980) to measure the absolute quantum yields of the FR-GECI solutions.

We performed pH titrations by diluting protein into buffers (pH from 2 to 11) containing 30 mM trisodium citrate, 30 mM sodium borate, 30 mM MOPS, 100 mM KCl, 10 mM EGTA, and either no CaCl$_2$ or 10 mM CaCl$_2$. Fluorescence intensities as a function of pH were then fitted by a sigmoidal binding function to determine the apparent pKa. Ca^{2+} titrations were carried out using Calcium

calibration buffer (Calcium Calibration Buffer Kit, Biotium, 59100). Fluorescence intensities against Ca^{2+} concentrations were fitted by a sigmoidal binding function to determine the Hill coefficient and K_d.

Wide-field calcium imaging in rat hippocampal neuron culture

The pAAV-hSyn-NIR-GECO-mut-IRES-EGFP-3NLS plasmid was transfected into cultured rat hippocampal neurons as described above. To analyze sensor brightness in neurons, more than 50 cells were snapshotted in mIFP/GFP channel for each mutant. 3–10 cells for each mutant were stimulated to fire 1–10 AP by patch clamp and the calcium ion flux was recorded simultaneously. To stimulate firing of 1–10 individual action potential (AP), 1–10 300-pA current pulses were injected to cultured neurons for 10 ms duration at a repetition rate of 50 Hz under I-CLAMP NORMAL mode (at 21159.48 Hz). The interval of each step from 1 to 10 AP was around 12 s. Fluorescence images were acquired at 48 Hz camera frame rate with 2-by-2 binning. neurons were illuminated with 637 nm laser at 3.3 W/cm^2.

QUANTIFICATION AND STATISTICAL ANALYSIS

Both the electrical data and the fluorescence images were analyzed with home-built scripts written in MATLAB R2018b (MathWorks). MATLAB code is available from Method S2. For neural calcium imaging, fluorescence intensities of cells were extracted from the mean pixel values of a manually drawn ROI around the soma. Following camera bias subtraction (100 and 400 for 1-by-1 and 2-by-2 binning, respectively), the fluorescence signal was corrected for photobleaching and smoothed by Savitzky-Golay filter. Statistical analysis was performed with Excel (Microsoft Excel 2019) and Origin (version 2022b).

Supplemental information

Functional imaging-guided cell selection

for evolving genetically encoded

fluorescent indicators

Chang Lin, Lihao Liu, and Peng Zou

Supplementary Table 1. The yield and precision of Faculae, related to Figure 1

Experiment	Number of Activated cells	Number of recovered PAmCherry⁺ cells	Yield	GFP⁺/ miRFP680⁻	GFP⁻/ miRFP680⁺	GFP⁻/ miRFP680⁻	Precision
#1	90	44	49%	40	1	3	91%
#2	50	19	38%	19	0	0	100%

Supplementary Table 2. Screening count of each library, related to Figure 2, 4 and 6

Library	Number of screened cells	Number of recovered PAmCherry⁺ cells	Number of sequencing results	Number of templates in result
miRFP680 library	0.4×10^5	48	17	12[a]
NIR-GECO1/2G mixed library	0.6×10^5	47	14	13[b]
mIFP library	1.1×10^5	43	22	8[b]
CaM library	1.0×10^5	36	15	7[b]
Combined library	1.2×10^5	81	21	0[b]
iBB library-R1	0.4×10^5	800	-[c]	-[c]
iBB library-R2	1.9×10^5	88	21	8[d]

[a] In this case, the template represents miRFP680. [b] In these cases, the template represents NIR-GECO2G. [c] In this case, cells were collected into one tube for PCR amplification of target gene. [d] In this case, the template represents Nier1s.

Supplementary Table 3. Characterization of FR-GECI mutants in HEK 293T, related to Figure 4

Mutants	Relative brightness[a]	Relative molecular brightness (normalized against EGFP)[a]	SBR[b]	Half time ($t_{1/2}$) of photobleaching (s)[c]
VNS (NIR-GECO2G)	1.00 ± 0.03	1.00 ± 0.02	1.00 ± 0.03	125 ± 4
QKM (Nier1s)	1.48 ± 0.05	1.47 ± 0.03	1.40 ± 0.10	155 ± 10
ETC (Nier1b)	2.55 ± 0.05	3.50 ± 0.11	1.00 ± 0.03	171 ± 11
STM	1.30 ± 0.12	1.67 ± 0.06	1.51 ± 0.08	132 ± 4
DRF	1.98 ± 0.06	1.81 ± 0.04	1.45 ± 0.10	141 ± 10
GCI	1.65 ± 0.08	1.70 ± 0.03	1.27 ± 0.09	150 ± 10
GRH	2.61 ± 0.16	2.82 ± 0.11	1.16 ± 0.05	142 ± 11
QRC	1.89 ± 0.13	2.77 ± 0.14	1.12 ± 0.04	-
KIV	2.41 ± 0.07	3.15 ± 0.06	1.05 ± 0.08	123 ± 11
RNP	2.99 ± 0.05	3.74 ± 0.06	1.04 ± 0.06	130 ± 6
KLA	2.41 ± 0.02	2.78 ± 0.11	1.04 ± 0.02	123 ± 3
KMC	2.83 ± 0.11	2.97 ± 0.07	1.03 ± 0.05	127 ± 8
TAA	1.81 ± 0.03	2.25 ± 0.11	1.03 ± 0.03	-
EEY	2.01 ± 0.13	2.60 ± 0.06	1.01 ± 0.04	-
NTT	1.86 ± 0.08	2.53 ± 0.05	1.00 ± 0.03	-
KSC	2.34 ± 0.14	3.11 ± 0.05	0.99 ± 0.05	130 ± 6

SRC	2.50 ± 0.06	2.84 ± 0.14	0.90 ± 0.05	147 ± 7
SHC	1.82 ± 0.06	2.98 ± 0.03	0.97 ± 0.07	-
DQV	3.43 ± 0.07	3.13 ± 0.04	0.96 ± 0.03	134 ± 5
QGV	2.80 ± 0.16	2.97 ± 0.06	0.88 ± 0.03	-
SGC	2.87 ± 0.23	2.72 ± 0.07	0.83 ± 0.05	-
RQP	2.74 ± 0.11	3.32 ± 0.05	0.73 ± 0.02	-

[a] Data were normalized to NIR-GECO2G. Each group contains three experimental replicates. Mean ± S.E.M

[b] Data were normalized to NIR-GECO2G. Each group contains 8-10 cells. Mean ± S.E.M

[c] Each group contains 8-10 cells. Mean ± S.E.M

Supplementary Table 4. Characterization of FR-GECI mutants in neuron, related to Figure 5

Mutants	Brightness rel. EGFP[a]	Response to 1 AP (%)[b]	Response to 10 AP (%)[b]	SNR (1AP) [b]	Half-rise time (1 AP) (ms) [b]	Half-decay time (1 AP) (s) [b]
VNS (NIR-GECO2G)	1.00 ± 0.10	-2.90 ± 0.53	-16.08 ± 2.24	11.57 ± 1.79	246 ± 17	1.46 ± 0.21
QKM (Nier1s)	1.22 ± 0.17	-5.77 ± 0.90	-23.03 ± 2.88	23.58 ± 4.00	227 ± 19	1.83 ± 0.21
ETC (Nier1b)	1.93 ± 0.24	-3.04 ± 0.62	-18.31 ± 1.32	18.75 ± 5.55	211 ± 19	1.05 ± 0.12
GRH	0.70 ± 0.14	-2.62 ± 0.62	-16.32 ± 1.99	9.55 ± 0.69	256 ± 34	1.50 ± 0.29
STM	1.20 ± 0.22	-2.91 ± 0.90	-16.25 ± 3.86	10.56 ± 4.23	331 ± 104	0.72 ± 0.15
GCI	1.21 ± 0.14	-3.60 ± 1.13	-18.16 ± 3.08	17.12 ± 4.90	207 ± 17	1.71 ± 0.30
DRF	1.23 ± 0.18	-2.81 ± 0.29	-20.70 ± 1.83	14.83 ± 1.58	241 ± 7	1.58 ± 0.10
RNP	1.67 ± 0.15	-1.95 ± 0.24	-9.97 ± 0.95	10.88 ± 3.08	303 ± 118	1.38 ± 0.43

[a] Data were normalized to NIR-GECO2G. VNS: 105 cells; QKM: 59 cells; ETC: 79 cells; GRH: 46 cells; STM: 33 cells; GCI: 99 cells; DRF: 53 cells; RNP: 88 cells. Mean ± S.E.M

[b] VNS: 10 cells; QKM: 10 cells; ETC: 10 cells; GRH: 5 cells; STM: 4 cells; GCI: 5 cells; DRF: 3 cells; RNP: 3 cells. Mean ± S.E.M

Supplementary Table 5. Characterization of NIR-GECI mutants in vitro, related to Figure 5

Indicator Name	[Ca^{2+}] (µM)	Ex (nm)	Em (nm)	EC (M^{-1}×cm^{-1})	QY (%)	Brightness (EC*QY)	pKa	K$_d$ (nM)	Hill Coeff. (n)
Nier1s	0	681	697	63000	3.3	2.1	5.8	146	0.96
	39	681	691	17000	0.52	0.088	4.2		
Nier1b	0	681	698	76000	4.4	3.3	4.8	308	0.91
	39	681	693	22000	3.3	0.73	4.2		
NIR-GECO2G	0	680	697	69000	3.0	2.1	5.4	194	0.94
	39	681	691	14000	1.3	0.18	4.1		

Supplementary Table 6. Characterization of Nier1s mutants in HEK 293T, related to Figure 6

Mutants	Relative brightness[a]	SBR[b]
Nier1s	1.00 ± 0.03	1.00 ± 0.03
Y271C	0.91 ± 0.02	0.98 ± 0.03
S373Y	1.54 ± 0.07	1.15 ± 0.02
S447D	0.79 ± 0.01	1.14 ± 0.09
323 △ GG/S447T	0.77 ± 0.02	1.14 ± 0.07
Y271F/I378T	1.24 ± 0.09	1.10 ± 0.03
E276D/Q428L	1.87 ± 0.07	0.90 ± 0.03
I378C	1.27 ± 0.09	1.01 ± 0.03
323 △ GG/S447N	0.77 ± 0.02	1.01 ± 0.02
323 △ GG	0.82 ± 0.04	1.06 ± 0.05

[a] Data were normalized to Nier1s. Each group contains two experimental replicates. Mean ± S.E.M

[b] Data were normalized to Nier1s. Each group contains 10 cells. Mean ± S.E.M

Supplementary Table 7. List of primers used in this study, related to STAR Methods

Primer name	Primer sequence (5'-3')
Head primer	ATGTCGGTACCGCTGACTACC
Tail primer	TTTGGACTGAGACTGTGCAAAGCTCTC
Forward primer-1	GCAACGTGCTGGTTATTGTGCTGTCTCATCATTTTG
Reverse primer-1	ACCCCTCCATGTGCACCTTGAAGCG
Forward primer-2	GGCAAAGAATTGGGGTTTGTCTGGTCAACC
Reverse primer-2	CCATGGATCCAGGGCCAGGGTTC
F60-F	GTTCCTGAACACCAACNNKGTTGTTGGCCGTCCGC
F60-R	GCGGACGGCCAACAACMNNGTTGGTGTTCAGGAAC
A125-F	GGAACCAGCAACCAAGNNKACTAACATTGCGCCGG
A125-R	CCGGCGCAATGTTAGTMNNCTTGGTTGCTGGTTCC
V133-F	CATTGCGCCGGCTCTGNNKGGTGCGCTTCATCGTA
V133-R	TACGATGAAGCGCACCMNNCAGAGCCGGCGCAATG
L136-F	GGCTCTGGTCGGTGCGNNKCATCGTATCACTTCTT
L136-R	AAGAAGTGATACGATGMNNCGCACCGACCAGAGCC
F156-F	CGAAACCGCGACTATTNNKCGTGAGATTACTGGCT
F156-R	AGCCAGTAATCTCACGMNNAATAGTCGCGGTTTCG
F162-F	CCGTGAGATTACTGGCNNKGACCGTGTGATGGTAA
F162-R	TTACCATCACACGGTCMNNGCCAGTAATCTCACGG
M168-F	CGACCGTGTGATGGTANNKCGTCTCGGCGCGCTTG
M168-R	CAAGCGCGCCGAGACGMNNTACCATCACACGGTCG
L353-F	CTCGCGTAGGCATGATNNKCTGTCCGAATGTCGTC
L353-R	GACGACATTCGGACAGMNNATCATGCCTACGCGAG
C357-F	TGATTTGCTGTCCGAANNKCGTCGTGCGGACCTGG
C357-R	CCAGGTCCGCACGACGMNNTTCGGACAGCAAATCA
Q377-F	GGCGTCTACTATTCCGNNKATCGCTCGTCGCCTGT
Q377-R	ACAGGCGACGAGCGATMNNCGGAATAGTAGACGCC
L385-F	TCGTCGCCTGTACGAANNKAACCGTGTTCGCCTGC
L385-R	GCAGGCGAACACGGTTMNNTTCGTACAGGCGACGA
E402-F	TACTCCGGTTCCGCTANNKCCGCGCATCAGCCCGC
E402-R	GCGGGCTGATGCGCGGMNNTAGCGGAACCGGAGTA
V455-F	TCTGTGGGGTCTGATCNNKTGCCACCACTACGAAC
V455-R	GTTCGTAGTGGTGGCAMNNGATCAGACCCCACAGA
Y463-F	CCACTACGAACCGCGCNNKGTTCCGTCCCACATTC
Y463-R	GAATGTGGGACGGAACMNNGCGCGGTTCGTAGTGG
S466-F	ACCGCGCTACGTTCCGNNKCACATTCGCGCTGCTG
S466-R	CAGCAGCGCGAATGTGMNNCGGAACGTAGCGCGGT

| A478-F	CGAAGCGCTGGCGGAANNKTGTGCGAACCGCATCG
A478-R	CGATGCGGTTCGCACAMNNTTCCGCCAGCGCTTCG
N481-F	GGCGGAAGCCTGTGCGNNKCGCATCGCGACGCTGG
N481-R	CCAGCGTCGCGATGCGMNNCGCACAGGCTTCCGCC
A319-F	TGTACAAATGATGACANNKAAGGGTGGCGGAGGTT
A319-R	AACCTCCGCCACCCTTMNNTGTCATCATTTGTACA
A342-F	GTCACGCAGTCAGANNKATAGGTCGGCTGGG
A342-R	CCCAGCCGACCTATMNNTCTGACTGCGTGAC
D283-F	TCGCCACGTGATGACANNKCTTGGTGAGAAGTTAA
D283-R	TTAACTTCTCACCAAGMNNTGTCATCACGTGGCGA
E291-F	TGAGAAGTTAACTGATNNKGAGGTTGATGAAATGA
E291-R	TCATTTCATCAACCTCMNNATCAGTTAACTTCTCA
F235-F	CGATGGCGACGGCATCNNKGACTTCCCTGAGTTCC
F235-R	GGAACTCAGGGAAGTCMNNGATGCCGTCGCCATCG
F237-F	CGACGGCATCTTCGACNNKCCTGAGTTCCTGACGA
F237-R	TCGTCAGGAACTCAGGMNNGTCGAAGATGCCGTCG
G259-F	TGAAGAGGAAATTAGANNKGCGTTCCGCGTGTTTG
G259-R	CAAACACGCGGAACGCMNNTCTAATTTCCTCTTCA
G273-F	CGGCAATGGCTACATCNNKGCAGCAGAGCTTCGCC
G273-R	GGCGAAGCTCTGCTGCMNNGATGTAGCCATTGCCG
G347-F	AGCTATAGGTCGGCTGNNKTCGCGTAGGCATGATT
G347-R	AATCATGCCTACGCGAMNNCAGCCGACCTATAGCT
I184-F	AGAGCAGATCGCAGAGNNKAAAGAGGCTTTCTCCC
I184-R	GGGAGAAAGCCTCTTTMNNCTCTGCGATCTGCTCT
I199-F	GGACGGGGACGGGACGNNKACAACCAAGGAGCTGG
I199-R	CCAGCTCCTTGGTTGTMNNCGTCCCGTCCCCGTCC
N249-F	GATGGCAAGGAAAATGNNKGACTCAGACAGTGAAG
N249-R	CTTCACTGTCTGAGTCMNNCATTTTCCTTGCCATC
N302-F	GATCAGGGTAGCAGACNNKGATGGGGATGGTCAGG
N302-R	CCTGACCATCCCCATCMNNGTCTGCTACCCTGATC
S251-F	AAGGAAAATGAATGACNNKGACAGTGAAGAGGAAA
S251-R	TTTCCTCTTCACTGTCMNNGTCATTCATTTTCCTT
T177-F	CGCGCTTGACGATCTGNNKGAAGAGCAGATCGCAG
T177-R	CTGCGATCTGCTCTTCMNNCAGATCGTCAAGCGCG
T206-F	AACCAAGGAGCTGGGGNNKGTGTTCCGGTCTCTGG
T206-R	CCAGAGACCGGAACACCGTCCCCAGCTCCTTGGTT
T289-F	CCTTGGTGAGAAGTTANNKGATGAGGAGGTTGATG
T289-R	CATCAACCTCCTCATCMNNTAACTTCTCACCAAGG
M223-F	AGCAGAGCTGCAGGACNNKATCAATGAAGTAGATG
M223-R	CATCTACTTCATTGATMNNGTCCTGCAGCTCTGCT

D232-F	AGTAGATGCCGATGGCNNKGGCATCTTCGACTTCC
D232-R	GGAAGTCGAAGATGCCMNNGCCATCGGCATCTACT
S251-F	AAGGAAAATGAATGACNNKGACAGTGAAGAGGAAA
S251-R	TTTCCTCTTCACTGTCMNNGTCATTCATTTTCCTT
Y271-F	TAAGGACGGCAATGGCNNKATCGGCGCAGCAGAGC
Y271-R	GCTCTGCTGCGCCGATMNNGCCATTGCCGTCCTTA
E276-F	CTACATCGGCGCAGCANNKCTTCGCCACGTGATGA
E276-R	TCATCACGTGGCGAAGMNNTGCTGCGCCGATGTAG
T282-F	GCTTCGCCACGTGATGNNKGACCTTGGTGAGAAGT
T282-R	ACTTCTCACCAAGGTCMNNCATCACGTGGCGAAGC
M316-F	CGAAGAGTTTGTACAANNKATGACAGCGAAGGGTG
M316-R	CACCCTTCGCTGTCATMNNTTGTACAAACTCTTCG
deltaGG-F	GACAGCGAAGGGTGGCTCTGTAGATTCATCAC
deltaGG-R	GTGATGAATCTACAGAGCCACCCTTCGCTGTC
GG-F	GACAGCGAAGGGTGGCGGAGGTTCTGTAGATTCATCAC
GG-R	GTGATGAATCTACAGAACCTCCGCCACCCTTCGCTGTC
S373-F	TAACCGCTACCCGGCGNNKACTATTCCGCAGATCG
S373-R	CGATCTGCGGAATAGTMNNCGCCGGGTAGCGGTTA
I378-F	GTCTACTATTCCGCAGNNKGCTCGTCGCCTGTACG
I378-R	CGTACAGGCGACGAGCMNNCTGCGGAATAGTAGAC
L391-F	TAACCGTGTTCGCCTGNNKGTAGATGTGAACTATA
L391-R	TATAGTTCACATCTACMNNCAGGCGAACACGGTTA
Y396-F	GCTGGTAGATGTGAACNNKACTCCGGTTCCGCTAG
Y396-R	CTAGCGGAACCGGAGTMNNGTTCACATCTACCAGC
Q428-F	TATGTCCCCGATCCACNNKAAATACATGCAGGACA
Q428-R	TGTCCTGCATGTATTTMNNGTGGATCGGGGACATA
S447-F	TTGCTCTCTGATGGTGNNKGGTCGTCTGTGGGGTC
S447-R	GACCCCACAGACGACCMNNCACCATCAGAGAGCAA

Supplementary Table 8. Plasmid catalog, related to STAR Methods

Plasmid	Description
pLX304-CAG-EBFP2-P2A-Bxb1-T2A-BSD	For CAG-LLP construction
pLX304-CMV-PAmCherry-P2A-miRFP680	Fig. 1d-f
pLX304-CMV-PAmCherry-P2A-EGFP	Fig. 1d-f
pLX304-CMV-PA-GFP	Fig. S2
attB-miRFP680-P2A-PAmCherry-NLS-EGFP-3NLS	For miRFP680 library construction
attB-EGFP	Fig. S3, S4
attB-mCherry	Fig. S3, S4
attB-NIR-GECO1 (2G)-3NLS-P2A-PAmCherry-NLS-sfGFP-3NLS	For NIR-GECO library construction. Fig. 3c-f
attB-GCaMP5g-NLS-IRES-dCherry	Fig. S7, S8
attB-GCaMP6s-NLS-IRES-mCherry	Fig. S7, S8
pcDNA3.1-NIRGECO2G-3NLS-P2A-EGFP-3NLS	For NIR-GECO characterization
pAAV-hSyn-NIR-GECO2G-IRES-EGFP-3NLS	For neural expression of NIR-GECO

Supplementary Table 9. Spectral properties and imaging apparatus for fluorescent imaging, related to STAR Methods

Indicator	Fluorophore	Excitation max. (nm)	Emission max. (nm)	Laser excitation wavelength (nm)	Emission filter (nm)
miRFP680	miRFP680	661	680	637	700 / 75
NIR-GECO	mIFP	683	704	637	700 / 75
EBFP2	EBFP2	383	448	405	460 / 50
mCherry	mCherry	587	610	561	630 / 75
EGFP	EGFP	489	508	488	525 / 50
GCaMP6s/GCaMP5g	cpEGFP	497	515	488	525 / 50
PAGFP	PAGFP (ON state)	504	517	488	525 / 50
PAmCherry	PAmCherry (ON state)	564	595	561	630 / 75
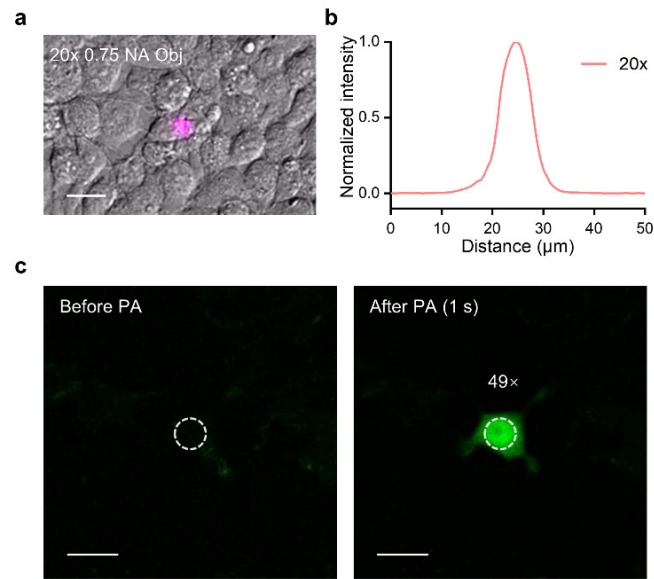
Supplementary Figure 1. Characterization of the focused spotlight for photoactivation, related to Figure 1. (A) The size of 405 nm spotlight under 20× 0.75 NA objective was determined by measuring spot size on the bottom of the glass dish. Scale bar: 20 μm. **(B)** The lateral distribution of the spot. **(C)** In cellular photoactivation of PAGFP using 405 nm focal illumination (1 s) resulted in large fluorescence change (49-fold). Dash line represents the estimated range of laser spot. Scale bar: 20 μm.
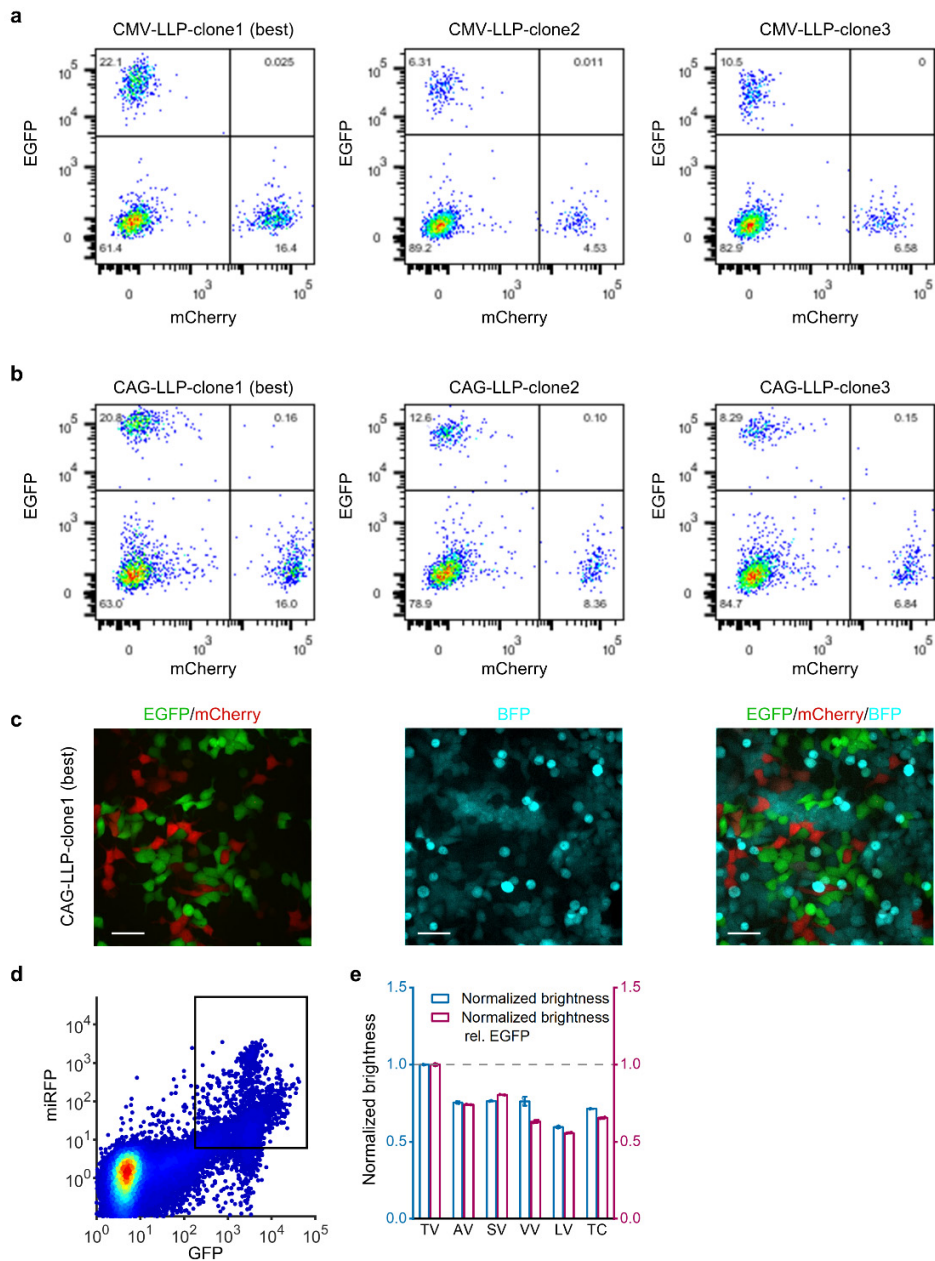
Supplementary Figure 2. Characterization of LLP cell line and miRFP680 mutants, related to Figure 2. (A-B) Characterization of LLP cell line clones. Representative cell line of CMV-LLP clones (a) and CAG-LLP clones (b) was transfected with the 1:1 plasmid mixture of attB-EGFP and attB-mCherry. The cells were analyzed by flow cytometry 3-4 days after transfection. **(C)** Fluorescent imaging of CAG-LLP-clone1 (best). In the co-transfection experiment, the recombined (BFP⁻) CAG-LLP cells exclusively express either EGFP or mCherry. Scale bar: 50 μm. **(D)** FACS analysis of miRFP680 library. Two days after transfection, miRFP680⁺/GFP⁺ cells (black gate, about 5%) were collected for further imaging-based screening. **(E)** Characterization of brightness for each miRFP680 mutant in HEK 293T. The brightness is normalized relative to TV. Two replicates in each group were analyzed by flow cytometry. Error bars represent S.E.M.
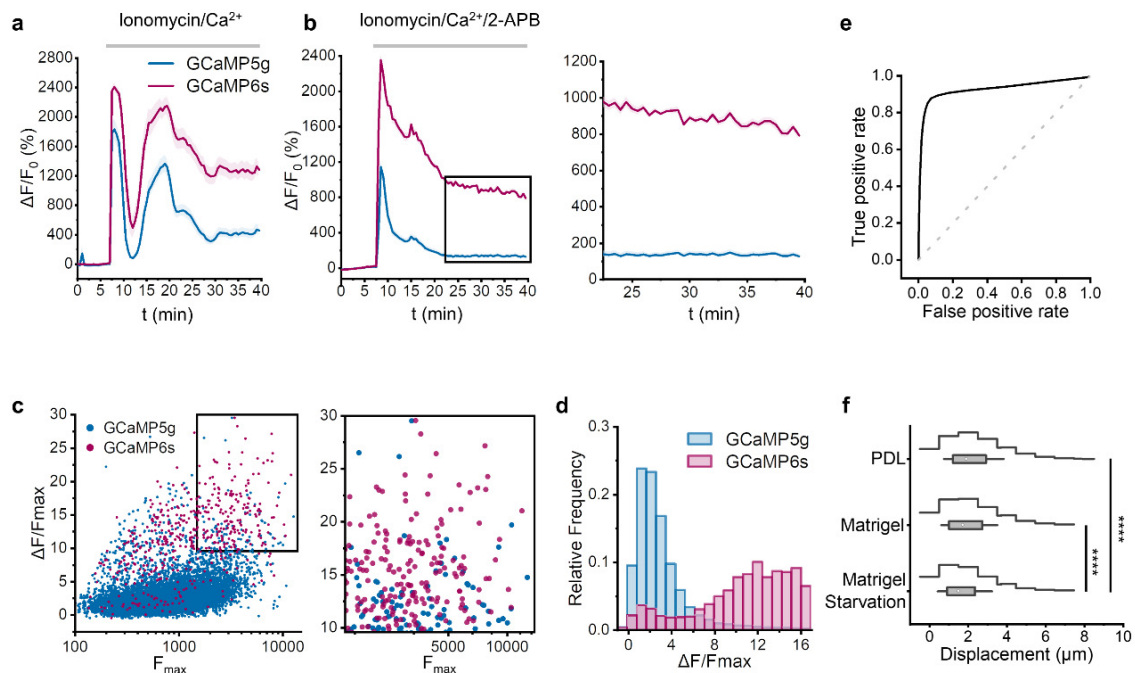
Supplementary Figure 3. Characterization of drug treatment assay, related to Figure 3. (A-B) Ionomycin/CaCl₂/2-APB Dosing strategy for increasing intracellular calcium level. HEK293T cells expressing either GCaMP5g-NLS-IRES-dCherry or GCaMP6s-NLS-IRES-mCherry were mixed (1:1) for time-lapse imaging. The buffer was changed 7 min after imaging started. **(A)** from EC to EC containing 2 µM Ionomycin and 1 mM CaCl₂. **(B)** from EC containing 50 µM 2-APB to EC containing 50 µM 2-APB, 2 µM Ionomycin and 1 mM CaCl₂. Right, zoomed trace from black frame in middle. 7-8 cells were counted for each group. Shaded areas represent S.E.M. **(C)** Model screening on GCaMP5g/GCaMP6s. HEK293T cells expressing either GCaMP5g-NLS-IRES-dCherry or GCaMP6s-NLS-IRES-mCherry were mixed (20:1) for two-round multi-position imaging (22×22 field of view). Brightness (F_{max}) and fluorescence change ((F_0-F_{max})/F_{max}) were calculated for each cell. Imaging buffer was changed from EC containing 50 µM 2-APB to EC containing 50 µM 2-APB, 2 µM Ionomycin and 1 mM CaCl₂. **(D)** The distribution of fluorescence change of GCaMP5g and GCaMP6s. **(E)** Receiver operating characteristic curve of GECI screening test. True positive rate (cell number of GCaMP6s/total cell number of GCaMP6s) and false positive rate (cell number of GCaMP6s/total cell number of GCaMP6s) were calculated at each fluorescence change from minimum to maximum. **(F)** Characterization of adherent cell migration under different treatment condition. HEK293T cells transfected with EGFP were seeded on pre-treated dishes to reach 70-80% confluence. Individual cells were tracked by imaging every 10 min. After 40 min, cell displacements were used for comparision. Data were analyzed by TrackMate (plugin in Fiji). PDL: PDL coated overnight, n_{cell} = 1173. Matrigel: Matrigel coated overnight, n_{cell} = 1538. Matrigel+Starvation: Matrigel coated overnight, serum starvation overnight, n_{cell} = 1167. **** represents p<0.0001. Boxes represent 25%~75% range. Error bars represent SD.

a

mIFP library

Number of mutation vs Targeted residues: 60, 125, 133, 136, 156, 162, 168, 353, 357, 377, 385, 402, 455, 463, 466, 478, 481

CaM library

Number of mutation vs Targeted residues: 177, 184, 199, 206, 235, 237, 249, 251, 259, 273, 283, 289, 291, 302, 319, 342, 347

b

Transfection — D0

1st FACS — D2

2nd FACS — D6

Imaging — D8

c

1st round FACS — GFP vs NIR-GECO, ~20%

2nd round FACS — GFP vs NIR-GECO, ~15%

d

mIFP library — $-\Delta F/F_0$ vs F_0

CaM library — $-\Delta F/F_0$ vs F_0

e

mIFP library

Sequence logo (Bits): F A V L F F M L C Q L E V Y S A N

NIR-GECO2G: F(60) A(125) V(133) L(136) F(156) F(162) M(168) L(353) C(357) Q(377) L(385) E(402) V(455) Y(463) S(466) A(478) N(481)

f

CaM library

Sequence logo (Bits): T I I T F N S G G D T E N A A G

NIR-GECO2G: T(177) I(184) I(199) T(206) F(235) F(237) N(249) S(251) G(259) G(273) D(283) T(289) E(291) N(302) A(319) A(342) G(347)

g

Normalized brightness rel. EGFP vs Normalized brightness. Tem.

h

$t_{1/2}$ (s) for: Tem, ETC, QKM, GCI, SRC, GRH, DRF, DQV, STM, RNP, KSC, KMC, KLA, KIV

Supplementary Figure 4. Characterization of mIFP library, CaM library and Combined library, related to Figure 4. (A) The distribution of mutation sites within mIFP library and CaM library of NIR-GECO2G. In each library, the distribution of mutations on selected sites was counted from 10 Sanger results. **(B)** Timeline of image-based pooled screening for FR-GECIs. **(C)** FACS analysis of mIFP library of NIR-GECO2G. The mIFP cell library was enriched by FACS twice. Black gates represent enriched cells. **(D)** Imaging-based screening result of mIFP library and CaM library of NIR-GECO2G. Black gates represent the range of selected cells (red scatter) for photoactivation. **(E-F)** Sequencing result and the sequence logo of screening result of mIFP **(E)** library and CaM **(F)** library from each recovered single cell. Sequencing results identical to the template were not included in the statistics. **(G)** HEK293T cells expressing NIR-GECO-mut-NLS-P2A-EGFP-NLS were analyzed by flow cytometry. The mean brightness value of each group was calculated from three biological replicates. Each mutant's brightness was normalized to template (NIR-GECO2G). **(H)** Photobleaching test of each mutant. HEK293T cells expressing NIR-GECO-mut-NLS-P2A-EGFP-NLS were illuminated by 637 nm at 9.0 W/cm^2. n_{cell} = 5-10 for each mutant. Error bars represent S.E.M.
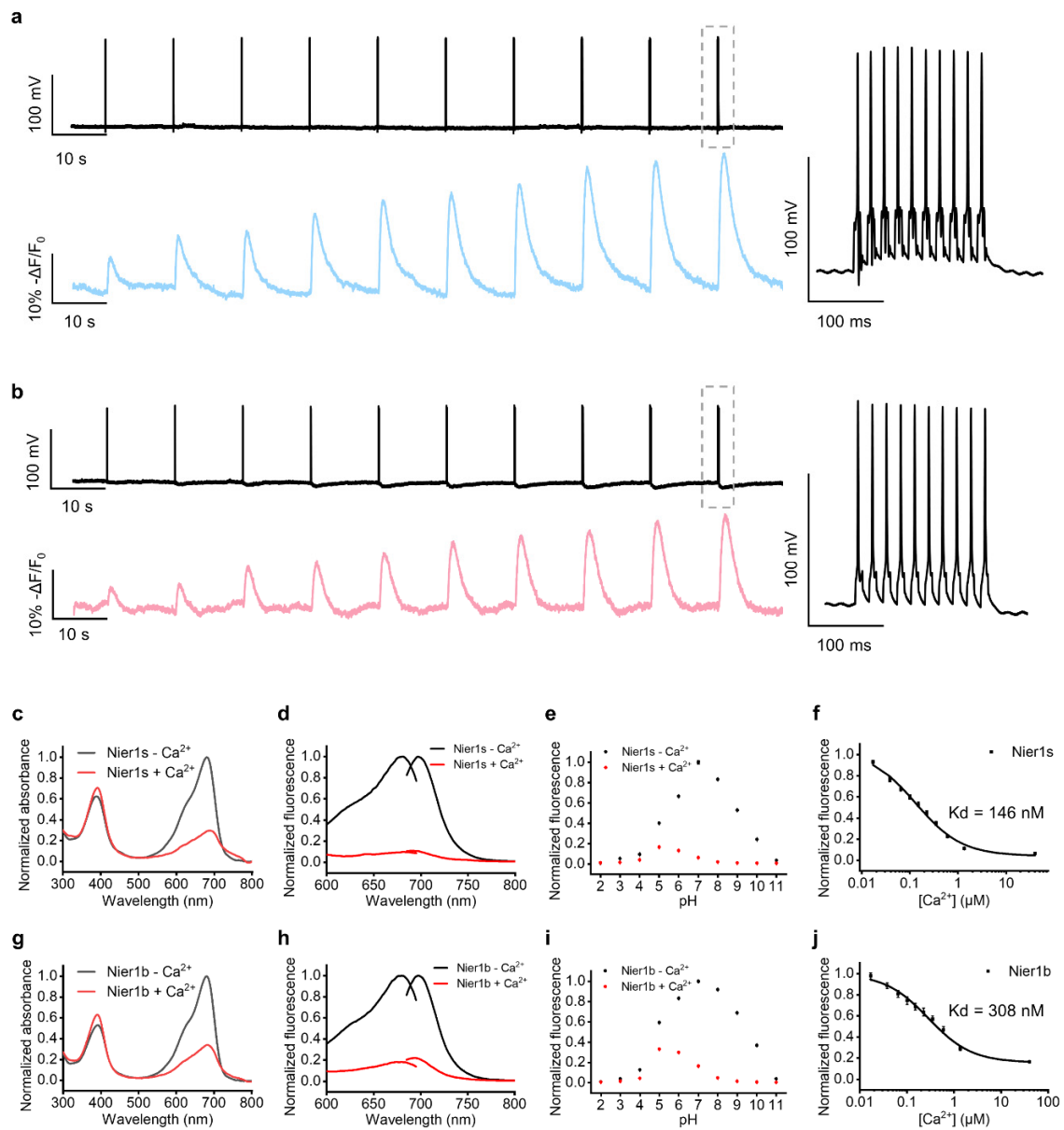
Supplementary Figure 5. Characterization of Nier1s and Nier1b in neurons and *in vitro*, related to Figure 5. (A-B) Representative electrophysiological traces and fluorescence traces of Nier1s-expressing neuron **(A)** or Nier1b-expressing neuron **(B)** in response to current injection (1 to 10 AP). The fluorescence traces were photobleaching calibrated. **(C-J)** Absorbance spectra of Nier1s **(C)** and Nier1b **(G)** in the presence (39 μM) and absence of Ca^{2+}. Fluorescence excitation and emission spectra of Nier1s **(D)** and Nier1b **(H)** in the presence (39 μM) and absence of Ca^{2+}. pH titration curves of Nier1s **(E)** and Nier1b **(I)** in the presence (39 μM) and absence of Ca^{2+}. $\triangle F/F_0$ of Nier1s **(F)** and Nier1b **(J)** as a function of Ca^{2+} concentration (mean ± SD, n = 2).

	M223L	D232N	S251A	Y271N	E276G	T282S	M316I	deltaGG		S373Y	I378T	L391M	Y396H	Q428L	S447F
NIR-GECO2G	M	D	S	Y	E	T	M	G	G	S	I	L	Y	Q	S
1.	M	D	S	Y	E	T	M	G	G	S	I	L	Y	Q	S
2.	M	D	S	Y	E	T	M	G	G	S	I	L	Y	Q	S
3.	M	D	S	Y	E	T	M	G	G	S	I	L	Y	Q	S
4.	M	D	S	Y	E	T	M	G	G	S	I	L	Y	Q	S
5.	M	D	S	Y	E	T	M	G	G	S	I	L	Y	Q	S
6.	M	D	S	Y	E	T	M	G	G	S	I	L	Y	Q	S
7.	M	D	S	Y	E	T	M	G	G	S	I	L	Y	Q	S
8.	M	D	S	Y	E	T	M	G	G	S	I	L	Y	Q	S
9.	M	D	S	Y	E	T	M	–	–	S	I	L	Y	Q	S
10.	M	D	S	Y	E	T	M	–	–	S	I	L	Y	Q	S
11.	M	D	S	Y	E	T	M	–	–	S	I	L	Y	Q	S
12.	M	D	S	Y	E	T	M	–	–	S	I	L	Y	Q	S
13.	M	D	S	Y	E	T	M	–	–	S	I	L	Y	Q	S
14.	M	D	S	Y	E	T	M	–	–	S	I	L	Y	Q	T
15.	M	D	S	Y	E	T	M	–	–	S	I	L	Y	Q	N
16.	M	D	S	Y	E	T	M	G	G	S	C	L	Y	Q	S
17.	M	D	S	F	E	T	M	G	G	S	C	L	Y	Q	S
18.	M	D	S	C	E	T	M	G	G	S	I	L	Y	Q	S
19.	M	D	S	Y	E	T	M	G	G	S	I	L	Y	Q	D
20.	M	D	S	Y	E	T	M	G	G	Y	I	L	Y	Q	S
21.	M	D	S	Y	D	T	M	G	G	S	I	L	Y	L	S

Supplementary Figure 6. Screening result of iBB library R2, related to Figure 6. Sequencing result of screening result of iBB library from each recovered single cell.

Method S1. MATLAB scripts for image-based FP/sensor screening, related to STAR Methods.

```
% this program is for library screens with stardist/cellpose process(dual channels), a typical experiment is
% selecting NIR-GECO mutants with higher brightness and sensitivity in 293T cells
% (LLP cell line express NIRGECO-3xNLS-P2A-PAmCherry-NLS-EGFP-3xNLS).
% For screens that need two channels, which
% including one marker channel(SDC-GFP in this case) and one library
% channel (SDC-Cy5 in this case), please set the marker channel as the
% first channel in MDA list while acquiring, otherwise this program will
% use wrong channel for calculating.
clear all;clc;
% [WARNING] the varient 'background' should be assigned as zero if flat field
% correction is proceed.

% This script is written by Chang Lin
%% MM FIJI Startup
simulate = 0;      % 0 for screening in A317, 1 for simulation on PC.
para_sensi = -1;   % -1 for negative going sensor, 1 for positive going sensor or unknown sensor
EdgeArea = 50;     % minimum area size (um2) 200 or 300 for cell membrane, 50 for nuclei
EdgeDis = 8;       % minimum edge distance (um) 10 for cell membrane, 8 for nuclei
EXP = 1;      % 1 for 200 ms exposure, 2 for 500 ms exposure time.
tem_sensi = 0.28;     % absolute value
if para_sensi == -1
    sensi_txt = '-';
else
    sensi_txt = ' ';
end
import org.micromanager.internal.MMStudio;
import mmcorej.*;
import org.micromanager.api.*;
import ij.*;
gui = MMStudio(false);    % start up MM2.0 gui within MATLAB
mmc = gui.getCore;   % get the MM2.0 CMMCore
acq = gui.getAcquisitionEngine; % org.micromanager.acquisition.internal.AcquisitionWrapperEngine
MDA = gui.getAcquisitionManager();
IJ = ij.IJ;
slm = gui.live();      % org.micromanager.internal.SnapLiveManager
Miji;     % start up FIJI within MATLAB
cd('C:\Users\ZouOptics\Desktop\MM2.0\code\matlab');
mmc.setConfig("System","Startup");
mmc.setConfig("System","Startup");    % this line repeat is necessary for 561/594 startup
```

```matlab
%% path selection
dir_flat = "C:\Users\ZouOptics\Desktop\MM2.0\flatfield\20230425";      % get direction of flat field on Z1
if simulate == 1
    dir_flat = "E:\pku\research_group\topic_screening_platform\flatfield\20220407";      % get direction of
flat field on PC
end
Channel_userdif = str2num(cell2mat(inputdlg({'Channel Num'},'input channel number',[1 35])))
switch(Channel_userdif)
    case{2}
        [file_flatMarker,path_flat] = uigetfile(dir_flat + "\*.*",'select bg-substrated Marker Channel flat field
image');
        file_flatMarker = string(file_flatMarker);
    case{1}
        file_flatMarker = [];
end
[file_flatLib,path_flat] = uigetfile(dir_flat + "\*.*",'select bg-substrated Library Channel flat field image');
file_flatLib = string(file_flatLib);
file_flat = [file_flatMarker file_flatLib];
[file_background1,path_flat] = uigetfile(dir_flat + "\*.*",'select marker channel black image');
[file_background2,path_flat] = uigetfile(dir_flat + "\*.*",'select library channel black image');
file_background = [string(file_background1) string(file_background2)];
% [file_ilastikModel,path_ilastikModel] = uigetfile(dir_ilastikModel + "\*.*",'select ilastik model');
path_flat = replace(path_flat,'\','/'); % for FIJI reading

%% spot ROI test and setting
% after acquisition, set up optical path and find the spot location,
% select the spot and run this section
IJ.runMacro("roiManager('reset');");
IJ.runMacro('roiManager("Add");');
MIJ.run("Set Measurements...", "area mean centroid stack redirect=None decimal=3");
IJ.runMacro("roiManager('Associate', 'true');");
IJ.runMacro('roiManager("Measure");');
spotROI = MIJ.getResultsTable();
IJ.runMacro("IJ.deleteRows(0,1);");
Xspot = spotROI(1,3);
Yspot = spotROI(1,4);
%% after configure, copy the dir_process to below
dir_process = "D:\LC_DATA\20230324_lin_CA31R2"; % get direction to process
dir = replace(dir_process,'\','/');
%% saving spot ROI
IJ.runMacro("roiManager('Select', 0);");
```

```
IJ.runMacro("roiManager('rename', 'laser spot');");
IJ.runMacro("roiManager('save selected', '" + dir +"/laser spot.zip"+ "');");
IJ.runMacro("roiManager('Deselect');");
IJ.runMacro("roiManager('Delete');");
clear spotROI;
%% please create grid and start the first round of screening
% for cellpose screening, use 20x20 or 22x22 grid
% for stardist screening, use 22x22 or 23x23 grid
% keep the MDA window open!!!
path_rawpre = dir_process + "\rawdata_pre";
mkdir(path_rawpre);
Channel_snap = strings(Channel_userdif,1);
for i = 1:Channel_userdif
list = {'SDC-LED','SDC-GFP','SDC-mCherry','SDC-Cy5'};
[indx,tf] = listdlg('PromptString',['Select channel_' num2str(i) ':'],...
                                'SelectionMode','single',...
                                'ListString',list);
Channel_snap(i) = list(indx);
end
pl_snap = gui.getPositionList(); % class org.micromanager.PositionList
Num_posi = pl_snap.getNumberOfPositions();
Num_grid = sqrt(Num_posi);
msp_snap = pl_snap.getPositions();
position_slice = zeros(Num_posi,3);
position_label = string(zeros(Num_posi,1));
XYStage_Label = msp_snap(1).getDefaultXYStage();
PFSStage_Label = msp_snap(1).getDefaultZStage();
PhysicalSize = double(mmc.getPixelSizeUm());
pl_snap.save(strcat(dir,'/screens.pos'));
for i = 1:Num_posi
    position_slice(i,1) = msp_snap(i).getX;
    position_slice(i,2) = msp_snap(i).getY;
    position_slice(i,3) = msp_snap(i).getZ;
    position_label(i,1) = msp_snap(i).getLabel();
end
for i = 1:Num_grid:Num_posi
    pl_snap.setPositions(msp_snap(i:i+Num_grid-1));
    if EXP == 1
        for j = 1:Channel_userdif

MDA.loadAcquisition('D:\Softwares\MM2.0\acqsetting\AcqSettings_'+Channel_snap(j)+'_multiP.txt');
```

```matlab
                MDA.runAcquisition(Channel_snap(j),path_rawpre);
                IJ.runMacro('close();');
            end
        else
            for j = 1:Channel_userdif

MDA.loadAcquisition('D:\Softwares\MM2.0\acqsetting\AcqSettings_'+Channel_snap(j)+'_multiP_500.txt');
                MDA.runAcquisition(Channel_snap(j),path_rawpre);
                IJ.runMacro('close();');
            end
        end
end
%% start the second round of screening
% after GECO screening(iono/Ca/2-APB), add drug and wait for 10-12 min before start the second round
of screening
% after GRAB screening(DA or AEA), add drug and wait for 7 min before start the second round of
screening
% after GEVI screening(GA), add drug and wait for ? min before start the second round of screening
path_rawpost = dir_process + "\rawdata_post";
mkdir(path_rawpost);
for i = 1:Num_grid:Num_posi
    pl_snap.setPositions(msp_snap(i:i+Num_grid-1));
    if EXP ==1
        for j = 1:Channel_userdif

MDA.loadAcquisition('D:\Softwares\MM2.0\acqsetting\AcqSettings_'+Channel_snap(j)+'_multiP.txt');
                MDA.runAcquisition(Channel_snap(j),path_rawpost);
                IJ.runMacro('close();');
            end
        else
            for j = 1:Channel_userdif

MDA.loadAcquisition('D:\Softwares\MM2.0\acqsetting\AcqSettings_'+Channel_snap(j)+'_multiP_500.txt');
                MDA.runAcquisition(Channel_snap(j),path_rawpost);
                IJ.runMacro('close();');
            end
        end
end
%% start the third round of screening if it is model screening
% mCherry/dCherry or EGFP/EGFP(Y66H)
[indx,tf] = listdlg('PromptString',['Select channel_model:'],...
```

```
                                    'SelectionMode','single',...
                                    'ListString',list);
Channel_model = list(indx);
path_rawmodel = dir_process + "\rawdata_model";
mkdir(path_rawmodel);
for i = 1:Num_grid:Num_posi
     pl_snap.setPositions(msp_snap(i:i+Num_grid-1));
     if EXP ==1
          MDA.loadAcquisition(['D:\Softwares\MM2.0\acqsetting\AcqSettings_' Channel_model{1}
'_multiP.txt']);
          MDA.runAcquisition(Channel_model{1},path_rawmodel);
          IJ.runMacro('close();');
     else
          MDA.loadAcquisition(['D:\Softwares\MM2.0\acqsetting\AcqSettings_' Channel_model{1}
'_multiP_500.txt']);
          MDA.runAcquisition(Channel_model{1},path_rawmodel);
          IJ.runMacro('close();');
     end
end
[file_model,path_model,indx] = uigetfile(path_rawmodel + "\*.*",'select model image');
for i = 1:Num_grid
     file_omeopen = strcat(Channel_model{1},'_',num2str(i),file_model(end-28:end-11),num2str(i-
1,"%03d"),file_model(end-7:end));
     path_omeopen = strcat(path_rawmodel,'\',Channel_model{1},'_',num2str(i),'\');
     MIJ.run("Bio-Formats", "open=[" + strcat(path_omeopen,file_omeopen) + "] color_mode=Default
concatenate_series open_all_series split_channels view=Hyperstack stack_order=XYCZT"); % open
"before" ome-tiff file
     IJ.runMacro("rename('"+Channel_model{1}+"_"+num2str(i)+"');");
end
Conc = 'image'+string([1:Num_grid]')+'=['+Channel_model{1}+'_'+string([1:Num_grid]')+']';
MIJ.run("Concatenate...",strcat("title=",Channel_model{1}," ",join(Conc,1)));
path_save = dir + "/channel_" + Channel_model{1};
mkdir(path_save);
MIJ.run("Image Sequence... ", "format=TIFF name=stack_ save=[" + path_save + "]");
%% process multi-channel multi-time-point ome-xml tiff
[file_ome,path_ome,indx] = uigetfile(path_rawpre + "\*.*",'select pre marker channel image');
[file_ome2,path_ome2,indx] = uigetfile(path_rawpost + "\*.*",'select post marker channel image');
for j =1:Channel_userdif
     for i = 1:Num_grid
          file_omeopen = strcat(Channel_snap(j),'_',num2str(i),file_ome(end-28:end-11),num2str(i-
1,"%03d"),file_ome(end-7:end));
```

```
        path_omeopen = strcat(path_rawpre,'\',Channel_snap(j),'_',num2str(i),'\');
        MIJ.run("Bio-Formats", "open=[" + strcat(path_omeopen,file_omeopen) + "] color_mode=Default
concatenate_series open_all_series split_channels view=Hyperstack stack_order=XYCZT"); % open
"before" ome-tiff file
        IJ.runMacro("rename('"+Channel_snap(j)+"_"+num2str(i)+"');");
    end
    Conc = 'image'+string([1:Num_grid]')+'=['+Channel_snap(j)+'_'+string([1:Num_grid]')+']';
    MIJ.run("Concatenate...",strcat("title=",Channel_snap(j)+'pre'," ",join(Conc,1)));
end
for j =1:Channel_userdif
    for i = 1:Num_grid
        file_omeopen = strcat(Channel_snap(j),'_',num2str(i),file_ome2(end-28:end-11),num2str(i-
1,"%03d"),file_ome2(end-7:end));
        path_omeopen = strcat(path_rawpost,'\',Channel_snap(j),'_',num2str(i),'\');
        MIJ.run("Bio-Formats", "open=[" + strcat(path_omeopen,file_omeopen) + "] color_mode=Default
concatenate_series open_all_series split_channels view=Hyperstack stack_order=XYCZT"); % open
"after" ome-tiff file
        IJ.runMacro("rename('"+Channel_snap(j)+"_"+num2str(i)+"');");
    end
    Conc = 'image'+string([1:Num_grid]')+'=['+Channel_snap(j)+'_'+string([1:Num_grid]')+']';
    MIJ.run("Concatenate...",strcat("title=",Channel_snap(j)+'post'," ",join(Conc,1)));
end
serialNum = Num_posi;
reader=bfGetReader([path_ome,file_ome]);
omeMeta = reader.getMetadataStore();
PixelsizeC =   omeMeta.getPixelsSizeC(0);
PixelsizeX = omeMeta.getPixelsSizeX(0);
PixelsizeY = omeMeta.getPixelsSizeY(0);
PhysicalSize = double(omeMeta.getPixelsPhysicalSizeX(0).value());
sizeC = double(PixelsizeC.getNumberValue());
sizeX = double(PixelsizeX.getNumberValue());
sizeY = double(PixelsizeY.getNumberValue());
clear indx PixelsizeC PixelsizeX PixelsizeY;

% flat field correction and generation of image sequence for each channel
Mean_flat = zeros(1,size(file_flat,2));
MIJ.run("Set Measurements...", "area mean centroid stack redirect=None decimal=3");
for i = 1:size(file_flat,2)
    IJ.runMacro("open('"+path_flat+file_flat(i)+"');");
    MIJ.run("Select All");
    MIJ.run("Measure");
```

```
        flat_data = MIJ.getResultsTable();
        Mean_flat(i) = flat_data(2);
        IJ.runMacro("IJ.deleteRows(0,1);");
        IJ.runMacro("open('"+path_flat+file_background(i)+"');");
end
window_selected = MIJ.getListImages;
window_selected = string(window_selected);
window_selected(find(strncmp(window_selected,'Preview',7) == 1))= [];
temp_Channel = Channel_snap(:,ones(1,2))';
Channel = reshape(temp_Channel',numel(temp_Channel),1);
Channel = strcat(Channel,["-before" "-before" "-after" "-after"]');
% process "before" and "after" image
for no= 1:size(Channel,1)
        MIJ.run("Calculator Plus", "i1=["+window_selected(no)+"] i2=["+file_background(2-mod(no,2))+"]
operation=[Subtract: i2 = (i1-i2) x k1 + k2] k1=1 k2=0 create");
        MIJ.selectWindow(window_selected(no));
        IJ.runMacro('close();');
        MIJ.selectWindow("Result");
        MIJ.run("Properties...", "channels=1 slices=1 frames="+num2str(serialNum)+" unit=micron
pixel_width="+num2str(PhysicalSize)+" pixel_height="+num2str(PhysicalSize)+" voxel_depth=1.0000000
frame=[0.00 sec]");
        IJ.runMacro("rename('"+Channel(no)+"');");
        MIJ.run("Calculator Plus", "i1=["+Channel(no)+"] i2=["+file_flat(2-mod(no,2))+"] operation=[Divide: i2
= (i1/i2) x k1 + k2] k1="+Mean_flat(2-mod(no,2))+" k2=0 create");
        MIJ.selectWindow(Channel(no));
        IJ.runMacro('close();');
        MIJ.selectWindow("Result");
        MIJ.run("Properties...", "channels=1 slices=1 frames="+num2str(serialNum)+" unit=micron
pixel_width="+num2str(PhysicalSize)+" pixel_height="+num2str(PhysicalSize)+" voxel_depth=1.0000000
frame=[0.00 sec]");
        IJ.runMacro("rename('"+Channel(no)+"');");
        if no<=2
            path_save = dir + "/channel_" + Channel(no,1);
        else
            path_save = dir + "/channel_" + Channel(no,1);
        end
        mkdir(path_save);
        MIJ.run("Image Sequence... ", "format=TIFF name=stack_ save=[" + path_save + "]");
end;
for i = 1:size(file_flat,2)
        MIJ.selectWindow(file_flat(i));
```

```matlab
        IJ.runMacro('close();');
        MIJ.selectWindow(file_background(i));
        IJ.runMacro('close();');
end
%% run stardist in a new FIJI window (for stardist screening)
% import post marker channel bg-substracted image sequence by bioformat, be
% sure that the t axis is set as the third axis. run stardist using default parameters and save the ROIs.
% [[NOTE]] you can reduce "persentile high" to 99 to eliminate the overexpressed cells

%% run cellpose in anaconda powershell prompt (for cellpose screening)
% conda activate cellpose
[file_cellpose,path_cellpose,indx] = uigetfile(dir_process + "\*.*",'select processed post-marker images for
segmentation');
system(['C:\Users\ZouOptics\anaconda3\envs\cellpose\python -m cellpose'...
    ' --dir ' [path_cellpose]...
    ' --pretrained_model cyto --chan 0 --use_gpu --fast_mode --save_png --no_npy --verbose']);
% open the processed image in a new FIJI by bioformat, then use
% "Plugins-BIOP-Image Analysis-ROIs-Label Image to ROIs" to get the ROI.
% saving the ROIs as .zip
%   --diameter 30
%% process stardist/cellpose returned result for confocal
[file_pro,path_pro,indx_pro] = uigetfile(dir_process + "\*.*",'select processed RoiSet');
MIJ.run("ROI Manager...");
IJ.runMacro("roiManager('reset');");
IJ.runMacro("roiManager('Open','"+replace(path_pro,'\','/') + file_pro+"');");
ResultsTable = cell(size(Channel,1),1);
IJ.runMacro('roiManager("count");');
MIJ.selectWindow("Log");
roiManagerSize = str2num(MIJ.getLog());
MIJ.run("Close" );
% IJ.runMacro("roiManager('save', '" + dir +"/libraryROI.zip"+ "');");
for no= 0:size(Channel,1)-1
    MIJ.selectWindow(Channel(no+1));
    %IJ.runMacro('roiManager("translate", 1, 0);');
    IJ.runMacro('roiManager("Measure");');
    ResultsTable(no+1,1) = {MIJ.getResultsTable()};
    IJ.runMacro("IJ.deleteRows(0, "+roiManagerSize+");");
end
MeanIntMarker_before = ResultsTable{1,1}(:,2);
MeanIntLib_before = ResultsTable{2,1}(:,2);
MeanIntMarker_after = ResultsTable{3,1}(:,2);
```

```matlab
MeanIntLib_after = ResultsTable{4,1}(:,2);
Area = ResultsTable{1,1}(:,1);
Slice = ResultsTable{1,1}(:,5);
Xrev = ResultsTable{1,1}(:,3);
Yrev = ResultsTable{1,1}(:,4);
Xabs = zeros(roiManagerSize,1);
Yabs = zeros(roiManagerSize,1);
Zabs = zeros(roiManagerSize,1);
camera = string(omeMeta.getDetectorID(0,0));
if camera == "camera_confocal"
    theta = atan(16/(2454-512));      %camera confocal# num calculated from file G:\lc
data\20210227_LC_dish\dish test 2\CELL_8\\CELL_7_MMStack_1-Pos000_000.ome.tif
else
    theta = 0;    %camera widefield unknown
end
Xcor = Xrev-Xspot;
Ycor = Yrev-Yspot;
Xcor_rev = Xcor*cos(theta)+Ycor*sin(theta);
Ycor_rev = Ycor*cos(theta)-Xcor*sin(theta);
Xabs = position_slice(Slice,1)+Xcor_rev;
Yabs = position_slice(Slice,2)+Ycor_rev;
Zabs = position_slice(Slice,3);
Sensitivity = (MeanIntLib_after./MeanIntMarker_after-
MeanIntLib_before./MeanIntMarker_before)./(MeanIntLib_before./MeanIntMarker_before);
PAstate = ones(roiManagerSize,1); % 1 refers to unlabeled, 2 refers to labeled, 3 refers to discard
Index = [1:roiManagerSize]';
AnalysisTable =
table(Index,Area,Slice,Xrev,Yrev,Xcor_rev,Ycor_rev,Zabs,MeanIntMarker_before,MeanIntLib_before,Mea
nIntMarker_after,MeanIntLib_after,Sensitivity,PAstate);
clear Index Area Slice Xrev Yrev Xcor_rev Ycor_rev Zabs MeanIntMarker_before MeanIntLib_before
MeanIntMarker_after MeanIntLib_after Sensitivity PAstate ResultsTable Xabs Yabs Xcor Ycor;
rows = (AnalysisTable.Area<EdgeArea | AnalysisTable.Xrev<EdgeDis |
AnalysisTable.Xrev>sizeX*PhysicalSize-EdgeDis | AnalysisTable.Yrev<EdgeDis |
AnalysisTable.Yrev>sizeX*PhysicalSize-EdgeDis);
AnalysisTable = AnalysisTable(~rows,:);
%% find ROIgate (brightness)
figure();hold;
if para_sensi == 1
    Xscatter = AnalysisTable.MeanIntMarker_after;
    Yscatter = AnalysisTable.MeanIntLib_after; % use "MeanIntLib_after" for positive-going sensor
else
```

```matlab
        Xscatter = AnalysisTable.MeanIntMarker_before;
        Yscatter = AnalysisTable.MeanIntLib_before; % use "MeanIntLib_before" for negative-going sensor
end
scatter(Xscatter,Yscatter,'Marker','.');
xlabel('Marker brightness');
set(gca, 'XScale', 'log');
set(gca, 'YScale', 'log');
title('select a gate');
ylabel('Library brightness');
gate = drawpolygon;
set(gate,'userdata',[Xscatter Yscatter]);
position_gate = customWait(gate);
in = inpolygon(log(Xscatter),log(Yscatter),log(position_gate(:,1)),log(position_gate(:,2)));
close(gcf);
figure();
plot(Xscatter(in),Yscatter(in),'r.',Xscatter(~in),Yscatter(~in),'b.');hold on
drawpolygon('Position',position_gate);
xlabel('Marker brightness');
set(gca, 'XScale', 'log');
set(gca, 'YScale', 'log');
title('select a gate');
ylabel('Library brightness');
title(gca,['Selected cell num:',num2str(sum(in))]);
path_Analysis = dir_process + "/Analysis";
mkdir(path_Analysis);
saveas(gca,path_Analysis+'/0 gating result.fig');
saveas(gca,path_Analysis+'/0 gating result.png');
BrightTable = AnalysisTable(in,:);
PATable = [];
clear in;
%% find ROIgate
% if you are evolving a sensor from a template without trying to reverse it, e.g. negative going NIR-GECO,
% positive going GRAB or negative going Ace2N-mNeon, run this section.
figure();hold;
if para_sensi == 1
        Xscatter = BrightTable.MeanIntLib_after;
else
        Xscatter = BrightTable.MeanIntLib_before; % use "MeanIntLib_before" for negative-going sensor
end
Yscatter = para_sensi*BrightTable.Sensitivity;
scatter(Xscatter,Yscatter,'Marker','.');
```

```matlab
plot([min(Xscatter),max(Xscatter)],[para_sensi*tem_sensi,para_sensi*tem_sensi],'r--');
xlabel('Library brightness');
set(gca, 'XScale', 'log');
title('select a gate');
ylabel(strcat('Sensitivity (',sensi_txt,'\DeltaF/F)'));
gate = drawpolygon;
set(gate,'userdata',[Xscatter Yscatter]);
position_gate = customWait(gate);
in = inpolygon(log(Xscatter),Yscatter,log(position_gate(:,1)),position_gate(:,2));
close(gcf);
figure();
plot(Xscatter(in),Yscatter(in),'r.',Xscatter(~in),Yscatter(~in),'b.');hold on
plot([min(Xscatter),max(Xscatter)],[para_sensi*tem_sensi,para_sensi*tem_sensi],'r--');
drawpolygon('Position',position_gate);
xlabel('Library brightness');
set(gca, 'XScale', 'log');
title('select a gate');
ylabel(strcat('Sensitivity (',sensi_txt,'\DeltaF/F)'));
title(gca,['Selected cell num:',num2str(sum(in))]);
saveas(gca,path_Analysis+'/1-1 gating result.fig');
saveas(gca,path_Analysis+'/1-1 gating result.png');
PATable = BrightTable(in,:);
clear in;
%% generate position list
pl = gui.getPositionList(); % class org.micromanager.PositionList
pl.clearAllPositions();
XYStage_Label = mmc.getXYStageDevice();
PFSStage_Label = 'TIPFSOffset'; % for stage1 in A317 , use 'TIPFSOffset',for demo use 'Z'
if simulate == 1
    PFSStage_Label = 'Z';
end
msp = cell(size(PATable,1),1);
for i = 1:size(PATable,1)
PosiX = position_slice(PATable.Slice(i),1)+PATable.Xcor_rev(i);
PosiY = position_slice(PATable.Slice(i),2)+PATable.Ycor_rev(i);
PosiZ = position_slice(PATable.Slice(i),3);
msp(i,1) = org.micromanager.MultiStagePosition(XYStage_Label,PosiX,PosiY,PFSStage_Label,PosiZ);
msp{i,1}.setLabel(['cell_',num2str(PATable.Index(i))]);
pl.addPosition(msp{i,1});
end
%% save analysis data
```

```matlab
save(path_Analysis+'/LibAnalysis.mat','AnalysisTable','BrightTable','PATable');
xlswrite(path_Analysis+'/LibAnalysis.xlsx',[AnalysisTable.Properties.VariableNames;table2cell(AnalysisTable)],'AnalysisTable');
xlswrite(path_Analysis+'/LibAnalysis.xlsx',[PATable.Properties.VariableNames;table2cell(PATable)],'PATable');
xlswrite(path_Analysis+'/LibAnalysis.xlsx',[BrightTable.Properties.VariableNames;table2cell(BrightTable)],'BrightTable');
%%   run PA_manually
run PA_manually_sensor_screen;
%% functions
function pos = customWait(hROI)
title('adjust your gate');
% Listen for mouse clicks on the ROI
l = addlistener(hROI,'ROIClicked',@clickCallback);
l = addlistener(hROI,'ROIMoved',@movedCallback);
% Block program execution
uiwait;

% Remove listener
delete(l);

% Return the current position
pos = hROI.Position;

end

function clickCallback(~,evt)

if strcmp(evt.SelectionType,'double')
    uiresume;
end

end

function movedCallback(src,evt)
coordinate = get(src,'userdata');
in = inpolygon(log(coordinate(:,1)),coordinate(:,2),log(src.Position(:,1)),src.Position(:,2));
title(gca,['Selected cell num:',num2str(sum(in))]);
end
```

Method S2. MATLAB scripts for patch analysis of FR-GECIs, related to STAR Methods.

```
% patch analysis for NIR-GECO. this script is for finding AP peaks from DAQ
% data and calculate the Ca sensitivity of GECI.
% reference: stimulated AP multicycles
clear all; clc;
%% load and select
% Movie loading path
dir_process = 'D:\lc_data\20221018_LIN_CAV24\A7\cell2\';
dire = -1;   % dire = 1 means positive GECI; dire = -1 means negative GECI
peak_thres = 20;      % mV

pathname = uigetdir(dir_process,'Select patch-imaging subfolder');
listing = dir(pathname);
for i =1:size(listing,1)
    if listing(i).isdir == 1 && ~strcmp(listing(i).name,'.')   && ~strcmp(listing(i).name,'..') &&
exist([pathname '\' listing(i).name '\matlab variables.mat'])
        load ([pathname '\' listing(i).name '\matlab variables.mat']);
        break
    end
end
if exist([dir_process '\patch param.txt'])
    b = importdata([dir_process '\patch param.txt']);
    datab = b.data;Cm = datab(1,5);Rm = datab(1,4);Ra = datab(1,3);%pF

else
    Rm = 'N.A.';Cm = 'N.A.';Ra = 'N.A.';
end

if exist([pathname '\movie_info.txt'])
    c = importfile([pathname '\movie_info.txt']);
elseif exist([pathname '\movie.txt'])
    c = importfile([pathname '\movie.txt']);
end
movname = '\movie.bin';
ncol = c.DO(find(strncmp(c.laser,'nrow',4) == 1));            % x invert
```

```matlab
nrow = c.DO(find(strncmp(c.laser,'ncol',4) == 1));              % y invert
camera_bias = c.DO(find(strncmp(c.laser,'Binning',7) == 1)).^2*100;   % background due to camera bias
(100 for bin 1x1)
dt_mov = c.DO(find(strncmp(c.laser,'Exposure',8) == 1));        % exposure time in millisecond (484 Hz)
Fs = samprate;
DAQname = '\movie_DAQ.txt';
dnsamp = Fs/(1000/dt_mov);            % downsampling rate = DAQ rate/camera rate
dnsamp = round(dnsamp);

% load DAQ data
tmp = importdata([pathname DAQname]);      % import data
data = tmp.data;                           % get array
Vm = data(:,2)*100;                        % Vm in millivolt, column vector
dt_daq = dt_mov/dnsamp;                    % DAQ dt in millisecond
t_daq = [0:length(Vm)-1]*dt_daq/10^3;      % DAQ time axis in second
a=importdata([pathname '\movie_DAQ.txt']);
data=a.data;
AI_scaled=data(:,1);
AI_10Vm=data(:,2)*100;
time=(1:length(AI_scaled)')'./Fs;
figure;
set(gcf,'outerposition',get(0,'screensize'));
plot(time,AI_scaled,time,AI_10Vm);
legend('AI\_scaled','Vm (mV)','Location','Northeast');
hold on
xlim=[0,max(time)];
ylim=[-70,-60];
xL=xlim;yL=ylim;
set(gca,'xtick',[0:5:max(time)])
box off
axis([xL yL])
axis tight
saveas(gca,[pathname '\0 waveform of AI.fig']);
saveas(gca,[pathname '\0 waveform of AI.png']);

%% loading the video movie
```

```matlab
% load movie
fname = [pathname movname];
[mov, nframe] = readBinMov(fname, nrow, ncol);
mov = single(mov);img = mean(mov, 3);
img,camera_bias,max(img,[],'all'), 'Please select interested regions');
[~, intens_raw] = clicky(mov, img, 'select only 1 ROI, right click when done');
intens_rembkg = intens_raw(:,1)-intens_raw(:,2);
% select ROI for analysis
background = mean(intens_raw(:,size(intens_raw,2)));

saveas(gca,[pathname '\1 clicky analysis.fig']);
saveas(gca,[pathname '\1 clicky analysis.png']);
len = size(intens_raw,1);
t_mov = [0:(len-1)]*dt_mov/1000;        % time axis in second

%% dump kernel by left click on axes
h = figure('Name','dump kernel by left click on axes');
set(gcf,'Position',get(0,'ScreenSize'));
ax = {};dumpIndex = ones(1,cycles);
headPts_fluo = size(headPts,2)/dnsamp;      tailPts_fluo = size(tailPts,2)/dnsamp;
bleachPts =   2*samprate/dnsamp;      cyclePts = (hiPts+lowPts)/dnsamp;
for i = 1:cycles
    kernel_Vm(1:hiPts+lowPts,i) = AI_10Vm(size(headPts,2)+(i-1)*(hiPts+lowPts)-
round(2*samprate)+1:size(headPts,2)+i*(hiPts+lowPts)-round(2*samprate));
    kernel_Fluo_dump(1:cyclePts,i) = intens_raw(headPts_fluo+(i-1)*cyclePts-
round(bleachPts)+1:headPts_fluo+i*cyclePts-round(bleachPts));
    ax{2*i-1} = subplot(cycles,2,2*i-1);      plot([0:hiPts+lowPts-1],kernel_Vm(:,i));
    ax{2*i} = subplot(cycles,2,2*i);      plot([0:cyclePts-1],kernel_Fluo_dump(:,i));
    if i<cycles
        set(ax{2*i-1},'xticklabel',[]);      set(ax{2*i},'xticklabel',[]);
    end

end
hold on
set(h.Children,'buttondownfcn',{@buttondownfcn,cycles,ax,pathname});          % assign function to
gca
```

```matlab
saveas(h,[pathname '\2 dumped kernel.fig']);
saveas(h,[pathname '\2 dumped kernel.png']);
%% photobleaching correction
% exponential fitting on remained kernels
intens_rembkg_norm = intens_rembkg./mean(intens_rembkg(1:round(headPts_fluo/100)));
plot(t_mov,intens_rembkg_norm');
F = @(x,xdata) x(1).*exp(-x(2).*xdata) + x(3).*exp(-x(4).*xdata);
x0 = [0.9 0.004 0.1 0.0001];
period_dataPts = [ones(1,round(bleachPts)), zeros(1,cyclePts-round(bleachPts))];
period_dataPts_false = [zeros(1,round(bleachPts)), zeros(1,cyclePts-round(bleachPts))];
% Cycle each period to give steps
dataPts = [ones(1,round(headPts_fluo)-round(bleachPts))];
for i = 1:cycles
if logical(dumpIndex(i))
    dataPts = [dataPts period_dataPts];
else
    dataPts = [dataPts period_dataPts_false];
end
end
dataPts = [dataPts zeros(1,round(bleachPts)) ones(1,round(tailPts_fluo))];
xdata = t_mov(logical(dataPts)); ydata = double(intens_rembkg_norm(logical(dataPts))');
x = lsqcurvefit(F,x0,xdata,ydata)
hold on
plot(t_mov,F(x,t_mov));
hold off
saveas(gca,[pathname '\3_1 photobleaching correction.fig']);
saveas(gca,[pathname '\3_1 photobleaching correction.png']);
close(gcf);
intens_corr = intens_rembkg_norm./F(x,t_mov)';
plot(t_mov,intens_rembkg_norm./F(x,t_mov)');
saveas(gca,[pathname '\3_2 trace after photobleaching correction.fig']);
saveas(gca,[pathname '\3_2 trace after photobleaching correction.png']);
%% calculate Ca deltaF/F versus AP number
% generate kernel
figure()
tkernel_Vm = repmat([0:hiPts+lowPts-1]*dt_daq/10^3,cycles,1)';
```

```matlab
tkernel_Fluo = repmat([0:cyclePts-1]*dt_mov/10^3,cycles,1)';
locs_Vpeak = {};
Num_Vpeak = [];
for i = 1:cycles
kernel_Fluo(1:cyclePts,i) = intens_corr(headPts_fluo+(i-1)*cyclePts-
round(bleachPts)+1:headPts_fluo+i*cyclePts-round(bleachPts));
[~,locs] = findpeaks(kernel_Vm(:,i),'MinPeakHeight',peak_thres);
Num_Vpeak=[Num_Vpeak size(locs,1)];
locs_Vpeak{i} = locs;

end
kernel_Fluo_smo = smoothdata(kernel_Fluo,1,'sgolay',30);
if dire == 1
    FluoPeak = max(kernel_Fluo_smo,[],1);
elseif dire == -1
    FluoPeak = min(kernel_Fluo_smo,[],1);
end
FluoSteady = mean(kernel_Fluo_smo(1:round(bleachPts),:),1);
SensiPeak = (FluoPeak-FluoSteady)./FluoSteady;
FluoPeak_half = (FluoPeak+FluoSteady)./2;
kernel_Fluo_norm = kernel_Fluo./FluoSteady;
kernel_Fluo_smo_norm = kernel_Fluo_smo./FluoSteady;
SNR = abs(FluoPeak-FluoSteady)./std(kernel_Fluo(round(bleachPts)-
round(bleachPts*0.25):round(bleachPts),:),1);
thalf_rise = [];
thalf_decay = [];
for i = 1:cycles
    if dumpIndex(i) == 1
        subplot(cycles,1,i);
        plot(tkernel_Fluo(:,i),kernel_Fluo_norm(:,i),tkernel_Fluo(:,i),kernel_Fluo_smo_norm(:,i));
        hold on
        Peak_Pt = find(kernel_Fluo_smo(:,i)==FluoPeak(i));
        if dire == -1
            thalf_rise_Pt = min(find(kernel_Fluo_smo(round(bleachPts)+1:Peak_Pt(1),i) <=
FluoPeak_half(i)));
            thalf_decay_Pt = min(find(kernel_Fluo_smo(Peak_Pt(1):end,i) >= FluoPeak_half(i)));
```

```
            else
                thalf_rise_Pt = min(find(kernel_Fluo_smo(round(bleachPts)+1:Peak_Pt(1),i) >=
FluoPeak_half(i)));
                thalf_decay_Pt = min(find(kernel_Fluo_smo(Peak_Pt(1):end,i) <= FluoPeak_half(i)));
            end
            thalf_rise = [thalf_rise thalf_rise_Pt*dt_mov];
            thalf_decay = [thalf_decay thalf_decay_Pt*dt_mov];

plot(tkernel_Fluo(round(bleachPts)+thalf_rise_Pt,i),kernel_Fluo_smo_norm(round(bleachPts)+thalf_rise_
Pt,i),'r.');
                plot(tkernel_Fluo(Peak_Pt(1)+thalf_decay_Pt-
1,i),kernel_Fluo_smo_norm(Peak_Pt(1)+thalf_decay_Pt,i),'r.');
            hold off
        else
            thalf_rise = [thalf_rise NaN];
            thalf_decay = [thalf_decay NaN];
        end
    end
end
saveas(gca,[pathname '\4 norm kernel with thalf.fig']);
saveas(gca,[pathname '\4 norm kernel with thalf.png']);
figure()
plot(tkernel_Fluo(:,logical(dumpIndex)),kernel_Fluo_norm(:,logical(dumpIndex)));
saveas(gca,[pathname '\5-1 norm kernel stack.fig']);
saveas(gca,[pathname '\5-1 norm kernel stack.png']);
close(gcf)
figure()
plot(tkernel_Fluo(:,logical(dumpIndex)),kernel_Fluo_smo_norm(:,logical(dumpIndex)));
saveas(gca,[pathname '\5-1 norm smooth kernel stack.fig']);
saveas(gca,[pathname '\5-1 norm smooth kernel stack.png']);
close(gcf)
%%
Num_Vpeak_save = Num_Vpeak(logical(dumpIndex));
SensiPeak_save = SensiPeak(logical(dumpIndex));
thalf_rise_save = thalf_rise(logical(dumpIndex));
thalf_decay_save = thalf_decay(logical(dumpIndex));
SNR_save = SNR(logical(dumpIndex));
```

```matlab
save([pathname
'\analysis.mat'],'AI_10Vm','dumpIndex','FluoPeak','FluoSteady','intens_rembkg','intens_corr','kernel_Fluo','
kernel_Fluo_norm','kernel_Fluo_smo','kernel_Fluo_smo_norm','kernel_Vm','tkernel_Fluo','tkernel_Vm');
xlswrite([pathname '\analysis.xlsx'],{'AP No.','Peak
response','t_half_rise','t_half_decay','SNR','Ra','Rm','Cm'},'Raw','A1');
xlswrite([pathname '\analysis.xlsx'],Num_Vpeak_save,'Raw','A2');
xlswrite([pathname '\analysis.xlsx'],SensiPeak_save,'Raw','B2');
xlswrite([pathname '\analysis.xlsx'],thalf_rise_save,'Raw','C2');
xlswrite([pathname '\analysis.xlsx'],thalf_decay_save,'Raw','D2');
xlswrite([pathname '\analysis.xlsx'],SNR_save,'Raw','E2');
xlswrite([pathname '\analysis.xlsx'],Ra,'Raw','F2');
xlswrite([pathname '\analysis.xlsx'],Rm,'Raw','G2');
xlswrite([pathname '\analysis.xlsx'],Cm,'Raw','H2');

Num_Vpeak_uni = unique(Num_Vpeak(logical(dumpIndex)));
for i = 1:size(Num_Vpeak_uni,2)
    lo = (Num_Vpeak_save == Num_Vpeak_uni(i));
    SensiPeak_uni(i) = mean(SensiPeak_save(lo));
    thalf_rise_uni(i) = mean(thalf_rise_save(lo));
    thalf_decay_uni(i) = mean(thalf_decay_save(lo));
    SNR_uni(i) = mean(SNR_save(lo));
end
xlswrite([pathname '\analysis.xlsx'],{'AP No.','Peak
response','t_half_rise','t_half_decay','SNR'},'Average','A1');
xlswrite([pathname '\analysis.xlsx'],Num_Vpeak_uni','Average','A2');
xlswrite([pathname '\analysis.xlsx'],SensiPeak_uni','Average','B2');
xlswrite([pathname '\analysis.xlsx'],thalf_rise_uni','Average','C2');
xlswrite([pathname '\analysis.xlsx'],thalf_decay_uni','Average','D2');
xlswrite([pathname '\analysis.xlsx'],SNR_uni','Average','E2');
%% functions
function buttondownfcn(hobj,~,cycles,ax,pathname)
dumpIndex = evalin('base','dumpIndex');
for i = 1:cycles
    if isequal(ax{2*i-1}.Position,get(hobj,'Position')) | isequal(ax{2*i}.Position,get(hobj,'Position'))
        dumpIndex(i) = 0;
```

```matlab
            title(ax{2*i-1},'dumped kernel');
            title(ax{2*i},'dumped kernel');
        end
    end
% set(hobj.Parent,'userdata',dumpIndex);        % add this line insdie the function
disp(dumpIndex);
assignin('base','dumpIndex',dumpIndex);
saveas(hobj.Parent,[pathname '\2 dumped kernel.fig']);
saveas(hobj.Parent,[pathname '\2 dumped kernel.png']);
end
```